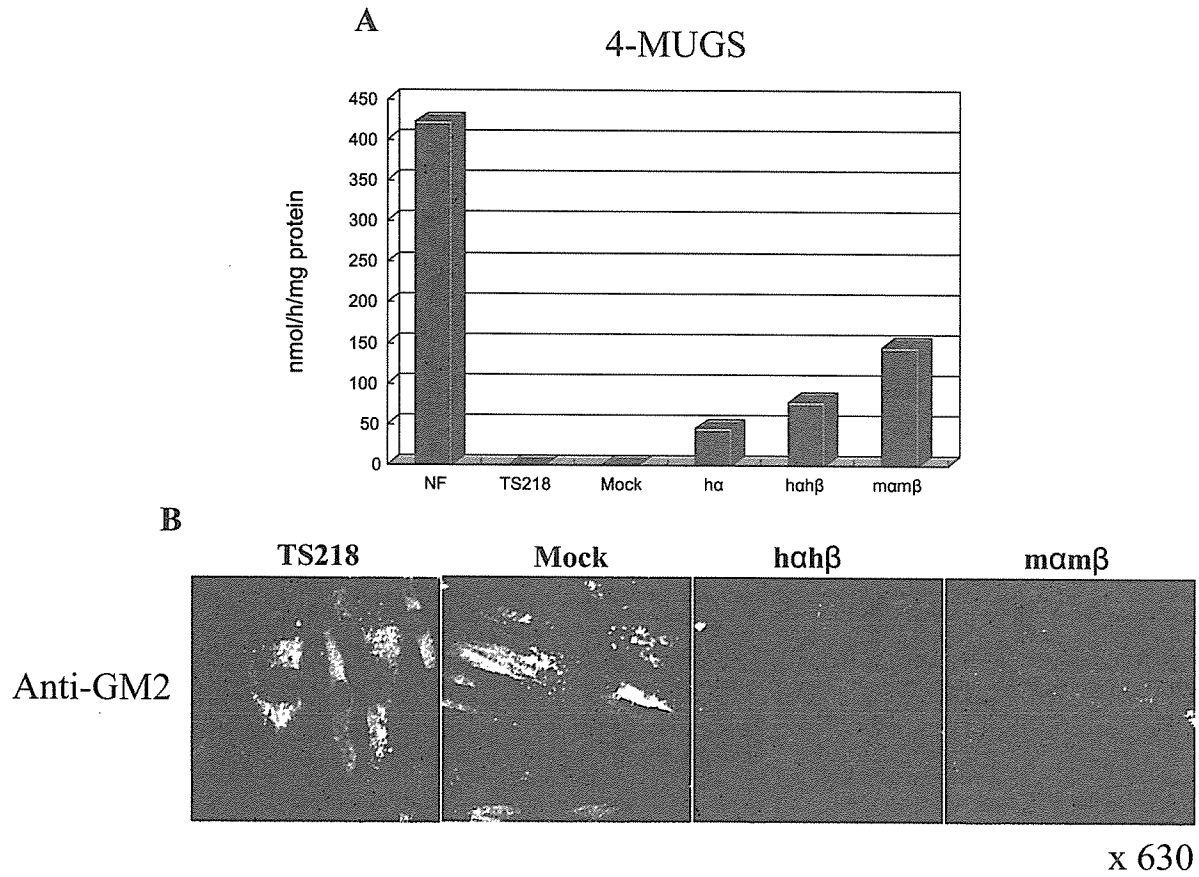

Fig. (6). Corrective effects of the recombinant Hex A on the accumulated natural substrates in Tay-Sachs fibroblasts.

Conditioned media containing a definite amount of 4-MUGS-degrading activity were added repeatedly to the culture medium of Tay-Sachs fibroblasts (TS218; 1~2 x 10^5 cells/60-mm dish). After 3 days culture, fibroblasts were harvested, and then Hex activities toward synthetic 4-MUGS in the cell extracts were measured (***A***). Each bar represents the mean for two independent experiments. (***B***) Degradation of intracellular GM2 ganglioside accumulated in Tay-Sachs fibroblasts (TS218) was evaluated by means of immunofluorescence with anti-GM2 ganglioside serum, and then a fluorescein-conjugated second antibody. Magnification, X 630. In panels: NF, normal fibroblasts; TS218, TS218 with the addition of conditioned medium from mock-transformed CHO; hα, conditioned medium from CHO-*HEXA*; hαhβ, conditioned medium from CHO-*HEXA/HEXB*; mαmβ, conditioned medium from CHO-*Hexa/Hexb*.

4-MUGS = 4-Methylumbelliferyl 6-sulfo-*N*-acetyl-β-D-glucosaminide

GlcNAc-oligosaccharides = Oligosaccharides carrying *N*-acetylglucosamine residues at their non-reducing termini

REFERENCES

[1] Sakuraba, H. http://www.glycoforum.gr.jp/science/word/glycopathology/GD- A05E.html.

[2] Raas-Roothscold, A.; Pankova-Kholmyansky, I.; Kacher, Y.; Futerman, A.H. *Glycoconj. J.* **2004**, *21*, 295.

[3] Guidotti, J.E.; Akli, S.; Casteinau-Ptakhine, L.; Kahn, A.; Poenaru, L. *Hum. Mol. Genet.* **1998**, *7*, 831

[4] Guidotti, J.E.; Haase, G.; Gaillaud, C.; McDonell, N.; Kahn, A.; Poenaru, L. *Hum. Mol. Genet.* **1999**, *8*, 831.

[5] Martino, S.; Cavalieri, C.; Emiliani, C.; Dolcetta, D.; Cusella De Angelis, M.G.; Chigorno, V.; Severini, G.M.; Sandhoff, K.; Bordignon, C.; Sonnino, S.; Orlacchio, A. *Neurochem. Res.* **2002**, *27*, 793.

[6] Jeyakumar, F.; Norflus, M.; Tifft, C.J.; Cortina-Borja, M.; Butters, T.D.; Proia, R.L.; Perry, V.H.; Dwek, R.A.; Platt, F.M. *Blood* **2001**, *97*, 327.

[7] Wada, R., Tifft, C.J.; Proia, R.L. *Proc. Natl. Acad. Sci. USA* **2000**, *97*, 10954.

[8] Grabowski, G.A.; Pastores, G., Brady, R.O.; Barton, N.W. *Pediatr. Res.* **1993**, *33*, 139A.

[9] Grabowski, G.A.; Barton, N.W.; Pastores, G.; Dambrosia, J.M.; Banerjee, T.K.; McKee, M.A.; Parker, C.; Schiffmann, R.; Hill, S.C.; Brady, R.O. *Ann. Intern. Med.* **1995**, *122*, 33.

[10] Schiffmann, R.; Murray, G.J.; Treco, D.; Daniel, P.; Sellos-Moura, M.; Myers, M.; Quirk, J.M.; Zirzow, G.C.; Borowski, M.; Loveday, K.; Anderson, T.; Gillespie, T.; Oliver, K.L.; Jeffries, N.O.; Doo, E.; Liang, T.J.; Kreps, C.; Gunter, K.; Frei, K.; Crutchfield, K.; Selden, R.F.; Brady, R.O. *Proc. Natl. Acad. Sci. USA* **2000**, *97*, 365.

[11] Schiffmann, R.; Kopp, J.B.; Austin, H.A.; Sabnis, S.; Moore, D.F.; Weibel, T.; Balow, J.E.; Brady, R.O. *J. Am. Med. Assoc.* **2001**, *285*, 2743.

[12] Eng, C.M.; Banikazemi, M.; Gordon, R.E.; Goldman, M.; Phelps, R.; Kim, L.; Gass, A.; Winston, J.; Dikman, S.; Fallon, J.T.; Brodie, S.; Stacy, C.B.; Mehta, D.; Parsons, R.; Norton, K.; O'Callaghan, M.; Desnick, R.J. *Am. J. Hum. Genet.* **2001**, *68*, 711.

[13] Eng, CM.; Guffon, N.; Wilcox, W.R.; Germain, D.P.; Lee, P.; Waldek, S.; Caplan, L.; Linthorst G.E.; Desnick, R. J. *N. Engl. J. Med.* **2001**, *345*, 9.

[14] Wraith, J.E.; Clarke, L.A.; Beck, M.; Kolodny, E.H.; Pastores, G.M.; Muenzer, J.; Rapoport, D.M.; Berger, K.I.; Swiedler, S.J.; Kakkis, E.D.; Braakman, T.; Chadbourne, E.; Walton-Bowen, K.; Cox, G.F. *J. Pediatr.* **2004**, *144*, 581.

[15] Klinge, L.; Straub, V.; Neudorf, U.; Schaper, J.; Bosbach, T.; Goerlinger, K.; Wallot, M.; Richards, S.; Voit, T. *Neuromuscul. Disord.* **2005**, *15*, 24.
[16] Van den Hout J.M.P.; Kamphoven, J.H.J.; Winkel, L.P.F.; Arts, W.F.M.; De Klerk, J.B.C.; Loonen, C.B.; Vulto A.G.; Cromme-Dijkhuis, A.; Weisglas-Kuperus, N.; Hop, W.; Van Hirtum, H.; Van Diggelen, O.P.; Boer, M.; Kroos, M.A.; Van Doorn, P.A.; Van der Voort, E.; Sibbles, B.; Van Corven, E.J.J.M.; Brakenhoff, J.P.J.; Van Hove, J.; Smeitink, J.A.M.; de Jong, G.; Reuser, A.J.J.; Van der Ploeg, A.T. *Pediatrics* **2004**, *113*, e448.
[17] Harmatz, P.; Whitley, C.B.; Waber, L.; Pais, R.; Steiner, R.; Plecko, B.; Kaplan, P.; Simon, J.; Butensky, E.; Hopwood, J.J. *J. Pediatr.* **2004**, *144*, 574.
[18] Muenzer, J.; Lamsa, J.C.; Garcia, A.; Dacosta, J.; Garcoa, J.; Treco, D.A. *Acta Paediatr. Suppl.* **2002**, *439*, 98.
[19] Gravel, R.A.; Kaback, M.M.; Proia, R.L.; Sandhoff, K.; Suzuki, K. In *The Metabolic and Molecular Bases of Inherited Disease, 8th* ed., Scriver, C.R.; Beaudet, A.L.; Sly, W.S.; Valle, D., eds.; McGraw-Hill: New York, **2001**; pp. 3827-3876.
[20] Mahuran, D.J. *Biochim. Biophy. Acta* **1999**, *1455*, 105.
[21] Kytzia, H. J.; Sandhoff, K. *J. Biol. Chem.* **1985**, *260*, 7568.
[22] Mark, B.L.; Mahuran, D.J.; Cherney, M.M.; Zhao, D.; Knapp, S.; James, M.N.G. *J. Biol. Chem.* **2003**, *327*, 1093.
[23] Maier, T.; Strator, N.; Schuette, C.G.; Klingenstein, R.; Sandhoff, K. *J. Mol. Biol.* **2003**, *328*, 669.
[24] Matsuzawa, F.; Aikawa, S.; Sakuraba, H.; Tanaka, A.; Ohno, K.; Sugimoto, Y.; Ninomiya, H.; Doi, H. *J. Hum. Genet.* **2003**, *48*, 582.
[25] Tanaka, A.; Pennett, H.H.; Suzuki, K. *Am. J. Hum. Genet.* **1990**, *47*, 567.
[26] Ohno, K.; Suzuki, K. *J. Neurochem.* **1988**, *50*, 316.
[27] Kytzia, H-J.; Hinrichs, U.; Maire, I.; Suzuki, K.; Sandhoff, K. *EMBO J.* **1983**, *2*, 1201.
[28] dos Santos, M.R.; Tanaka, A.; sa Miranda, C.; Ribero, M.G.; Maia, M.; Suzuki, K. *Am. J. Hum. Genet.* **1991**, *49*, 886.
[29] Tanaka, A.; Ohno, K.; Suzuki, K. *Biochem. Biophys. Res. Commun.* **1988**, *156*, 1015.
[30] Brown, C.A.; Neote, K.; Leung, A.; Gravel, R.A.; Mahuran, D.J. *J. Biol. Chem.* **1989**, *264*, 21706.
[31] Paw, B.H.; Moskowitz, S.M.; Uhrhammer, N.; Wright, N.; Kaback, M.M.; Neufeld, E.F. *J. Biol. Chem.* **1990**, *265*, 9452.
[32] Paw, B.H.; Wood, L.C.; Neufeld E.F. *Am. J. Hum. Genet.* **1991**, *48*, 1139.
[33] Kuroki, Y.; Itoh, K.; Nadaoka, Y.; Tanaka, T.; Sakuraba, H. *Biochem. Biophys. Res. Commun.* **1995**, *212*, 564.
[34] Hara, A.; Uyama, E.; Uchino, M.; Shimmoto, M.; Utsumi, K.; Itoh, K.; Kase, R.; Naito, M.; Sugiyama, E.; Taketomi, T.; Sukegawa, K.; Sakuraba, H. *J. Neurol. Sci.* **1998**, *155*, 86.
[35] Sakuraba H.; Matsuzawa, F.; Aikawa, S.; Doi, H.; Kotani, M.; Lin, H.; Ohno, K.; Tanaka, A.; Yamada, H.; Uyama, E. *J. Hum. Genet.* **2002**, *47*, 176.
[36] deDuve, C. *Fed. Proc.* **1964**, *23*, 1045.
[37] Barton, N.W.; Brady, R.O.; Dambrosia, J.M.; Di Bisceglie, A.M.; Doppelt, S.H.; Hill, S.C.; Mankin, H.J.; Murray, G.J.; Parker, R.I.; Argoff, C.E.; Grewal, R.P.; Yu, K-T. *N. Engl. J. Med.* **1991**, *324*, 1464.
[38] Kornfeld, S.; Sly, W.S. In *The Metabolic and Molecular Bases of Inherited Disease, 8th.* ed., Scriver, C.R.; Beaudet, A.L.; Sly, W.S.; Valle, D.S. eds,; McGraw-Hill: New York, **2001**; pp. 3469-3482.
[39] Lee, K.; Jin, X.Y.; Zhang, K.; Copertino, L.; Andrews, L.; Baker-Malcolm, J.; Geagen, L.; Qui, H.W.; Seiger, K.; Barngrover, D.; McPherson, J.M.; Edmunds, T. *Glycobiology* **2003**, *13*, 305.
[40] Hantzopoulos, P.A.; Calhoun, D.H. *Gene* **1987**, *57*, 159.
[41] Coppola, G.; Yan, Y.; Hantzopoulos, P.A.; Segura, E.; Stroh, J.G.; Calhoun, D.H. *Gene* **1994**, *144*, 197.
[42] Chen, Y.; Jin, M.; Egborge, T.; Coppola, G.; Andre, J.; Calhoun, D.H. *Prot. Expr. Purif.* **2000**, *20*, 472.
[43] Vinogradov, E.; Peterson, B.O.; Duus, J.O. *Carbohydr. Res.* **2000**, *325*, 216.
[44] Chiba, Y.; Sakuraba, H.; Kotani, M.; Kase, R.; Kobayashi, K.; Takeuchi, M.; Ogasawara, S.; Maruyama, Y.; Nakajima, T.; Takaoka,Y.; Jigami, Y. *Glycobiology* **2002**, *12*, 821.
[45] Nakanishi-Shindo, Y.; Nakayama, K.; Tanaka, A.; Toda, Y.; Jigami, Y. *J. Biol. Chem.* **1993**, *268*, 26338.
[46] Odani, T.; Shimma, Y.; Tanaka, A.; Jigami, Y. *Glycobiology* **1996**, *6*, 805.
[47] Tong, P.Y.; Gregory, W.; Kornfeld, S. *J. Biol. Chem.* **1989**, *264*, 7962.
[48] Akeboshi, H.; Kasahara, Y.; Tsuji, D.; Tatano, Y.; Itoh, K.; Sakuraba, H.; Chiba, Y.; Jigami, Y. *Seikagaku* **2004**, *76*, 1024.
[49] Sawada, M.; Suzumura, A.; Marunouchi, T. *Int. J. Dev. Neurosci.* **1995**, *13*, 253.
[50] Gehrmann, J.; Matsumoto, Y.; Kreutzberg, G.W. *Brain Res. Rev.* **1995**, *20*, 269.
[51] Kurihara, Y.; Matsumoto, A.; Itakura, H.; Kodama, T. *Curr. Opin. Lipidol.* **1991**, *2*, 295.
[52] Lassmann, H.; Schmied, M.; Vass, K.; Hickey, W.F. *Glia* **1993**, *7*, 19.
[53] Sawada, M.; Suzumura, A.; Yamamoto, H.; Marunouchi, T. *Brain Res.* **1990**, *509*, 119.
[54] Sawada, M.; Suzumura, A.; Marunouchi, T. *Biochem. Biophys. Res. Commun.* **1992**, *189*, 869.
[55] Sawada, M.; Suzumura, A.; Itoh, Y.; Marunouchi, T. *Neurosci. Lett.* **1993**, *155*, 175.
[56] Sawada, M.; Suzumura, A.; Marunouchi, T. *J. Neurochem.* **1995**, *64*, 1973.
[57] Suzumura, A.; Marunouchi, T.; Yamamoto, H. *Brain Res.* **1991**, *545*, 301.
[58] Ziegler-Heitbrock, H.W.L.; Ulevitch, R.J. *Immunol. Today* **1993**, *14*, 121.
[59] Horan, P.K; Slezak, S.E. *Nature* **1989**, *340*, 167.
[60] Melnicoff, M.J.; Horan, P.K.; Breslin, E.W.; Morahan, P.S. *J. Leukoc. Biol.* **1998**, *44*, 367.
[61] Ishihara, S.; Sawada, M.; Chang, L.; Kim, J.M.; Brightman, M. *Exp. Neurol.* **1993**, *124*, 219.
[62] Mulligan, R.C. *Science* **1993**, *260*, 926.
[63] Kozarsky, K.F.; Wilson, J.M. *Curr. Opin. Genet. Dev.* **1993**, *3*, 499.
[64] Nishi, T.; Yoshizato, K.; Yamashiro, S.; Takeshima, H.; Sato, K.; Hamada, K.; Kitamura, I.; Yoshimura, T.; Saya, H.; Kuratsu, J.; Ushio, Y. *Cancer Res.* **1996**, *56*, 1050.
[65] Yamanaka, S.; Johnson, O.N.; Norflus, F.; Boles, D.J.; Proia, R.L. *Genomics* **1994**, *21*, 588.
[66] Wakamatsu, N.; Benoit, G.; Lamhonwah, A.; Zhang, Z.X.; Trasler, J.M.; Raine, B.L.; Gravel, R.A. *Genomics* **1994**, *24*, 110.
[67] Martino, S.; Emiliani, C.; Tancini, B.; Severini, G.M.; Chigorno, V.; Bordignon, C.; Sonnino, S.; Orlacchio, A. *J. Biol. Chem.* **2002**, *277*, 20177.

Received: August 16, 2005 **Accepted: June 2, 2006**

Neuroscience 142 (2006) 87–96

THE INTRA-ARTERIAL INJECTION OF MICROGLIA PROTECTS HIPPOCAMPAL CA1 NEURONS AGAINST GLOBAL ISCHEMIA-INDUCED FUNCTIONAL DEFICITS IN RATS

Y. HAYASHI,[a] Y. TOMIMATSU,[a] H. SUZUKI,[b] J. YAMADA,[a] Z. WU,[a] H. YAO,[c] Y. KAGAMIISHI,[d] N. TATEISHI,[d] M. SAWADA[b] AND H. NAKANISHI[a]*

[a]*Laboratory of Oral Aging Science, Faculty of Dental Sciences, Kyushu University, Fukuoka 812-8582, Japan*

[b]*Department of Brain Life Science, Research Institute of Environmental Medicine, Nagoya University, Nagoya 464-8601, Japan*

[c]*Laboratory for Neurochemistry, Hizen National Hospital, Saga 342-0192, Japan*

[d]*Minase Research Laboratories, Ono Pharmaceutical Co., Ltd., Osaka 618-8585, Japan*

Abstract—In the present study, we have attempted to elucidate the effects of the intra-arterial injection of microglia on the global ischemia-induced functional and morphological deficits of hippocampal CA1 neurons. When PKH26-labeled immortalized microglial cells, GMIR1, were injected into the subclavian artery, these exogenous microglia were found to accumulate in the hippocampus at 24 h after ischemia. In hippocampal slices prepared from medium-injected rats subjected to ischemia 48 h earlier, synaptic dysfunctions including a significant reduction of synaptic responses and a marked reduction of long-term potentiation (LTP) of the CA3–CA1 Schaffer collateral synapses were observed. At this stage, however, neither significant neuronal degeneration nor gliosis was observed in the hippocampus. At 96 h after ischemia, there was a total loss of the synaptic activity and a marked neuronal death in the CA1 subfield. In contrast, the basal synaptic transmission and LTP of the CA3–CA1 synapses were well preserved after ischemia in the slices prepared from the microglia-injected animals. We also found the microglial-conditioned medium (MCM) to significantly increase the frequency of the spontaneous postsynaptic currents of CA1 neurons without affecting the amplitude, thus indicating that MCM increased the provability of the neurotransmitter release. The protective effect of the intra-arterial injected microglia against the ischemia-induced neuronal degeneration in the hippocampus was substantiated by immunohistochemical and immunoblot analyses. Furthermore, the arterial-injected microglia prevented the ischemia-induced decline of the brain-derived neurotrophic factor (BDNF) levels in CA1 neurons. These observations strongly suggest that the arterial-injection of microglia protected CA1 neurons against the ischemia-induced neuronal degeneration. The restoration of the ischemia-induced synaptic deficits and the resultant reduction of the BDNF levels in CA1 neurons, possibly by the release of diffusible factor(s), might thus contribute to the protective effect of the arterial-injection of microglia against ischemia-induced neuronal degeneration.

Key words: microglia, intra-arterial injection, global ischemia, hippocampal CA1 neurons, brain-derived neurotrophic factor, electrophysiology.

In response to pathological conditions including cerebral ischemia, ramified microglia rapidly transform into activated states and accumulate in pathological sites. When neurons are severely injured, the microglia further transform into phagocytic cells. It remains controversial whether the microglia which accumulate at pathological sites are harmful or beneficial. There is growing evidence that the activated microglia are harmful for the injured neurons associated with ischemia, while the inhibition of microglial activation could reduce ischemic brain injury (Lees, 1993). Lipid-soluble tetracyclines, doxycycline and minocycline, have been reported to inhibit microglial activation, while they also have a neuroprotective effect against global brain ischemia (Yrjänheikki et al., 1998). On the other hand, some studies have suggested that microglia might have a beneficial effect on ischemic injured neurons. The proliferation of microglia after ischemia has also been suggested to contribute to the ischemic tolerance (Liu et al., 2001).

The intra-cerebral introduction of microglia is one of the direct approaches to elucidate the role of microglia in the ischemic brain. Recently, Kitamura et al. (2004, 2005) examined the effects of i.c.v.-injected microglia on neurodegeneration induced by the middle cerebral artery occlusion (MCAO) and reperfusion. After MCAO, i.c.v.-injected microglia were found to accumulate in the infracted core in rat brain parenchyma. They performed histological and functional analyses to show a neuroprotective effect of exogenous microglia on neuronal injury induced by MCAO. Unfortunately, i.c.v.-injected microglia may induce several undesirable events such as the entry of blood cells to the ischemic lesions and immunologic responses, which complicate the analysis of the role of microglia. We have previously reported that microglial cell lines as well as primary cultured microglia retain the ability to enter the normal brain from the circulation (Imai et al., 1997; Sawada et al., 1998; Imai et al., 1999). Furthermore, intra-arterial-injected microglia migraded to the ischemic hippocampal CA1 sub-

*Corresponding author. Tel: +81-92-642-6413; fax: +81-92-642-6415.
E-mail address: nakan@dent.kyushu-u.ac.jp (H. Nakanishi).

Abbreviations: BDNF, brain-derived neurotrophic factor; CD, cathepsin D; CLSM, confocal laser-scanning microscope; FCS, fetal calf serum; GFAP, glial fibrillary acidic protein; Iba1, ionized calcium binding adaptor molecule 1; I–O, input–output; LTP, long-term potentiation; MAP2, microtubule-associated protein-2; MCAO, middle cerebral artery occlusion; MCM, microglial-conditioned medium; MEM, minimal essential medium; NeuN, neuronal nuclei; NMDA, *N*-methyl-D-aspartic acid; PBS, phosphate-buffered saline; pEPSP, population excitatory postsynaptic potential; PI, propidium iodide; rCBF, regional cerebral blood flow; SDS, sodium dodecyl sulfate.

0306-4522/06$30.00+0.00
doi:10.1016/j.neuroscience.2006.06.003

field, one of the most vulnerable neuronal populations against global forebrain ischemia (Imai et al., 1997, 1999). Therefore, the intra-arterial injection of microglia can be a suitable approach to address the question of whether microglia are harmful or beneficial to the ischemic neuronal injury.

In the present study, we have thus utilized this intra-arterial injection system and found that the arterial-injected microglia protected CA1 neurons against the ischemia-induced neuronal degeneration by a combination of electrophysiological and morphological analyses. The arterial-injected microglia ameliorated the ischemia-induced synaptic deficits and the resultant reduction of brain-derived neurotrophic factor (BDNF) levels in CA1 neurons possibly by releasing diffusible factor(s). These effects might contribute to the protective effect of the arterial-injection of microglia against the ischemia-induced neuronal degeneration.

EXPERIMENTAL PROCEDURES

Animals

This study was approved by the Animal Research Committee of the Kyushu University Faculty of Dental Sciences. The study was carried out using male Wistar rats weighing 180–210 g. The rats were housed in group cages under 12-h light/dark conditions and then were given free access to food and water. The experimental procedure was approved by the Animal Research Committee of the Kyushu University Faculty of Dental Sciences, and was conducted in accordance with the guidelines of the U.S. National Institutes of Health on the Care and Use of Laboratory Animals. Every effort was made to minimize the number of animals used and their suffering.

Cell culture

GMIR1, an immortalized microglial clone, was established from a rat primary microglial culture which has been described previously (Morihata et al., 2000; Salimi et al., 2002). GMIR1 cells displayed strong wheat germ agglutinin and IB4-lectin binding and immunoreactivity for antibodies recognizing OX-42 and ED1, indicating that this clone had microglial properties (Salimi et al., 2002). GMIR1 cells were cultured in Petri dishes in Eagle's minimal essential medium (MEM) containing 10% fetal calf serum (FCS), 0.2% glucose, 5 mg/l bovine insulin, pH 7.3 and supplemented with 1 ng/ml granulocyte-macrophage colony stimulating factor (Genzyme, Cambridge, MA, USA) at 37 °C in 5% CO_2. Before injection, the cells were tagged with a lipid-soluble fluorescent dye PKH-26 (Zynaxis, Malvern, PA, USA). PKH26-stained cells were harvested using a rubber policeman in 2 ml of ice-cold phosphate-buffered saline (PBS) which was centrifuged three times.

Preparation of peritoneal macrophages

Macrophages were collected by injecting 20 ml of cold (4 °C) PBS into the peritoneal cavities of male Wistar rats. Peritoneal fluid was withdrawn three times with a 21-gauge needle and a plastic syringe. The cells were kept at 4 °C, centrifuged at 1000×*g* for 5 min, and seeded onto plastic dishes containing MEM with 10% FCS. The non-adherent cells were removed after 2 h and the adherent macrophages were cultured for 24 h in MEM containing 10% FCS, where they were allowed for 1 h at 37 °C in 5% CO_2.

Microglial injection and forebrain ischemia

Male Wistar rats were anesthetized with halothane and the tagged microglial cells (2×10^6 cells in 500 μl of medium) were injected as a bolus over 30 s into the recipient's subclavian artery. In some experiments, microglia fixed with 4% paraformaldehyde or peripheral macrophages (2×10^6 cells in 500 μl of medium) were injected into the recipient's subclavian artery. Four to 7 days after injection, rats were subjected to transient forebrain ischemia by clamping the carotid arteries bilaterally according to the method of Pulsinelli and Brierley (1979). Briefly, the animals were anesthetized with the mixture of ketamine (50 mg/kg) and xylazine (10 mg/kg) and bilateral vertebral arteries were electrocauterized at the level of the first vertebra. On the following day, the common carotid arteries were gently exposed and both arteries were occluded with a vascular clamp for 10 min. The rectal temperature was maintained at 36.5–37.5 °C. The rats that had lost their righting reflexes during the period of ischemia were used as the postischemic group. This procedure induced a total loss of neurons in the hippocampal CA1 subfield of medium-injected rats assessed by Nissl staining and microtubule-associated protein-2 (MAP2)-immunohistochemistry. In a parallel set of experiments, the changes in the regional cerebral blood flow (rCBF) (1 mm posterior and 2–4 mm lateral to the bregma) were continuously monitored with a laser-Doppler flowmeter (ALF 21D, Advance Co. Ltd., Tokyo, Japan). The changes in the rCBF were expressed as a percentage of the average of two to three baseline values. After bilateral carotid occlusion, the rCBF decreased to 19.9% (range: 12.0–25.0%, number of animals=3) and 14.7% (range: 9.1–21.4%, number of animals=4) of the control values in the medium- and microglia-injected animals, respectively. The extents of rCBF reduction after carotid occlusion did not differ between the two groups.

Quantitative analysis of infiltrated cells

PKH26-labeled microglia-injected sham and animals subjected to 10-min of four-vessel occlusion 24 h and 48 h earlier (number of animals=3, each) were anesthetized with sodium pentobarbital (40 mg/kg, i.p.) and killed by intracardiac perfusion with isotonic saline followed by a chilled fixative consisting of 4% paraformaldehyde in 0.2 M PBS (pH 7.4). After perfusion, the brain was removed and further fixed by immersion in the same fixative overnight at 4 °C, and then immersed in 20% sucrose (pH 7.4) for 24 h at 4 °C. Serial parasagittal sections (10 μm thick) of the whole hippocampus were prepared by a cryostat. Three sections were randomly selected from each group. Images of PKH26-positive cells infiltrated in each section were taken as a stack at 1-μm step size along z-direction with a 20× objective by a confocal laser-scanning microscope (CLSM) (LSM510MET, Carl Zeiss, Jena, Germany) (Shimizu et al., 2005).

Electrophysiology

For electrophysiological analyses, postischemic slices were taken from either group subjected to 10-min of four-vessel occlusion 48 h (number of animals=5, each group), 96 h (number of animals=5, each group) and 1 week (number of animals=3) earlier. Sham slices were taken from medium- and microglia-injected animals subjected to identical surgical exposure without vessel occlusion 96 h (number of animals=3, each group) earlier. Animals of both the ischemic and sham groups were decapitated under light ether anesthesia and then were rapidly removed and placed in ice-cold Krebs Ringer solution of the following composition (in mM): NaCl 124.0, KCl 2.5, KH_2PO_4 1.24, $NaHCO_3$ 26.0, $CaCl_2$ 2.4, $MgSO_4$ 1.3 and glucose 10.0. Transverse hippocampal slices (thickness of 400 μm) ranging from 2.0–3.5 mm lateral to the midline were cut with a vibrating microtome (VT 1000S, Leica, Heidelberg, Germany) were used for electrophysiological studies. A single hippocampal slice was placed in an interface-type record-

ing chamber at a constant bath temperature of 32±0.1 °C. Electrical stimulation (intensity 0–40 V, duration 20 μs, frequency 0.3 Hz) was applied to Schaffer collateral afferents through a bipolar stainless steel electrode. The extracellular field potentials were recorded with a glass electrode filled with perfusate and placed on the stratum pyramidal or stratum radiatum of the CA1 subfield. Stimulus-response curves were constructed by using stimulus intensities from 0 to 40 V in increments of 5 V. The responses were subsequently set to a level that gave a slope value 20% of the maximum obtained. Baseline responses were obtained every 30 s. Paired-pulse facilitation was assessed using a succession of paired pulses separated by intervals of 25, 50, 100, 200, and 300 ms. An additional 30 min baseline period was obtained before attempting to induce long-term potentiation (LTP). LTP experiments were performed on transverse hippocampal slices as described previously (Tomimatsu et al., 2002). LTP was induced by tetanus stimulation, consisting of a train of pulses of 1 s duration with a tetanus at 100 Hz, given at the test stimulus intensity.

For whole cell recordings, transverse hippocampal slice (thickness of 400 μm) from male Wistar rats weighing 100–120 g were cut with a vibrating microtome (VT 1000S, Leica) in ice-cold Krebs Ringer solution. The slices were placed in an interface-type chamber at a constant bath temperature of 32±0.1 °C. Whole-cell recordings were obtained from CA1 pyramidal cells using blind patch clamp technique in the whole cell voltage clamp mode (EPC-9, HEKA, Lambrecht, Germany). Patch electrode of 4–7 MΩ from glass (outer diameter 1.5 mm, inner diameter 0.9 mm, WPI) were fabricated on a puller (Model P-97, Sutter Instruments, Novato, CA, USA). For recording spontaneous miniature currents, internal solution was composed of (in mM): $CsMeSO_3H$ 130, TEA-Cl 5, CsCl 5, EGTA 2, Hepes 10, $MgCl_2$ 1, ATP-Mg 4, and pH was adjusted to 7.4 with Tris-base. Series resistance was continuously monitored during recordings. All experiments were filtered at 2 kHz, digitized at 4 kHz and stored on a computer equipped with A/D converter (Power Laboratory). Spontaneous miniature currents were counted and analyzed using the MiniAnalysis program (Synaptosoft, Decatur, GA, USA). Spontaneous events were screened automatically using an amplitude threshold of 15 pA and then visually accepted or rejected based on the rise and decay times. The average values of frequency and amplitude of spontaneous miniature currents during the control period were calculated, and the frequency and amplitude of all the events during MCM application were normalized to these values.

Immunohistochemistry

For immunohistochemistry, animals subjected to 10-min of four-vessel occlusion 48 h (number of animals=3, each group), and 96 h (number of animals=3, each group) earlier were deeply anesthetized with sodium pentobarbital (100 mg/kg, i.p.) and then transcardially perfused with isotonic saline, followed by a chilled fixative consisting of 4% paraformaldehyde in 0.1 M phosphate buffer (pH 7.4). The brain was left *in situ* for 2 h at room temperature and then it was removed from the skull. Small blocks containing the hippocampus separated from the brain were further fixed by immersion in the same fixative overnight, cryoprotected overnight in 30% sucrose in PBS, and were then embedded in an optimal cutting temperature compound (Sakura Finetechnical Co., Ltd., Tokyo, Japan). Floating parasaggital sections (40 μm thick) of the hippocampus were prepared by a cryostat and stained with anti-MAP2 (1:1000) (Chemicon International, Temecula, CA, USA), anti-cathepsin D (CD, 5 μg/ml), anti-CD11b (1:200) (OX42, Serotec, Bichester, UK), anti-glial fibrillary acidic protein (1:1000) (GFAP, Chemicon International) or anti-ionized calcium binding adaptor molecule 1 (1:500) (Iba1, Wako Pure Chemical Industries, Inc., Osaka, Japan) antibodies for 3 days at 4 °C. Antisera to purified rat spleen CD was raised in rabbits and purified by affinity chromatography. After washing with PBS, the sections were incubated with biotinylated anti-goat or anti-horse IgG for 2 h at room temperature. After washing with PBS, the sections were incubated with streptavidin-Alexa 488 (Molecular Probes Inc., Eugene, OR, USA) for 2 h at room temperature. After washing with PBS, the sections were further stained with propidium iodide (PI, 5 μM/ml) (Sigma Chemical Company, St. Louis, MO, USA) for 5 min at room temperature. For double staining, floating sections were incubated with anti-BDNF (1:50) (Santa Cruz Biotechnology, Santa Cruz, CA, USA) and anti-neuronal nuclei (1:200) (NeuN, Chemicon International) antibodies for 3 days at 4 °C. After washing with PBS, the sections were incubated with a mixture of fluorescein isothiocyanate-conjugated donkey anti-rabbit IgG and rhodamine-conjugated donkey anti-mouse IgG for 1 h at room temperature. After several washes with PBS, the sections were mounted in the anti-fading medium Vectashield (Vector Laboratories, Burlingame, CA, USA) and then were examined with the CLSM (LSM510MET, Carl Zeiss). For the quantitative assessment of the immunofluorescence of BDNF, the immunofluorescence intensity was determined as the average pixel intensity in the CA1 subfield of the hippocampus.

Immunoblotting

For immunohistochemical analyses, the dorsal hippocampus was taken from either group subjected to 10-min of four-vessel occlusion 48 h (number of animals=3, each group), and 96 h (number of animals=3, each group) earlier. As the sham sample, the dorsal hippocampus was also taken from the medium- and microglia-injected animals subjected to identical surgical exposure without vessel occlusion 96 h (number of animals=3, each group) earlier. The animals were anesthetized by sodium pentobarbital anesthesia (40 mg/ml, i.p.) and killed by intracardiac perfusion with isotonic saline. The soluble fractions obtained from the hippocampus homogenates by differential centrifugation, as described below, were electrophoresed using sodium dodecyl sulfate (SDS)–polyacrylamide gels. Proteins on SDS gels were transferred electrophoretically at 100 V for 12–15 h from the gel to nitrocellulose membranes and then incubated at 4 °C overnight under gentle agitation with primary antibody against CD or MAP2. After washing, the membranes were incubated with 0.5% horseradish peroxidase–labeled donkey anti-rabbit IgG (Amersham, Buckinghamshire, UK). Subsequently, membrane-bound, HRP-labeled antibodies were detected by an enhanced chemiluminescence detection system kit (Amersham). As a control, the primary antibody was replaced by nonimmune rabbit IgG. The protein bands were scanned and analyzed densitometrically.

Preparation of microglial-conditioned medium (MCM)

Mixed glial cells were prepared from the cerebral cortex of 3-day-old Wistar rats and cultured in Eagle's MEM (Nissui Pharmaceutical Co., Tokyo, Japan) containing 10% fetal bovine serum (HyClone, Logan, UT, USA), 0.2% $NaHCO_3$, 2 mM glutamine, 0.2% glucose, 25 μg/ml insulin, 5000 U/ml penicillin and 5 mg/ml streptomycin according to the methods described previously (Moriguchi et al., 2003). After isolation, microglia were replaced in six-well plates (2×10^6/ml) and maintained in serum-free MEM containing 0.2% $NaHCO_3$, 2 mM glutamine, 0.2% glucose, 25 μg/ml insulin, 5000 U/ml penicillin and 5 mg/ml streptomycin. After 2 days in culture, supernatants were retrieved and filtered by 0.22-μm filter (Millex-GS, Millipore, Billerica, MA, USA) and stored at −80 °C.

Statistical analysis

The experimental values are shown as the mean±S.E. Statistical analyses of the results were evaluated using the Student's *t*-test.

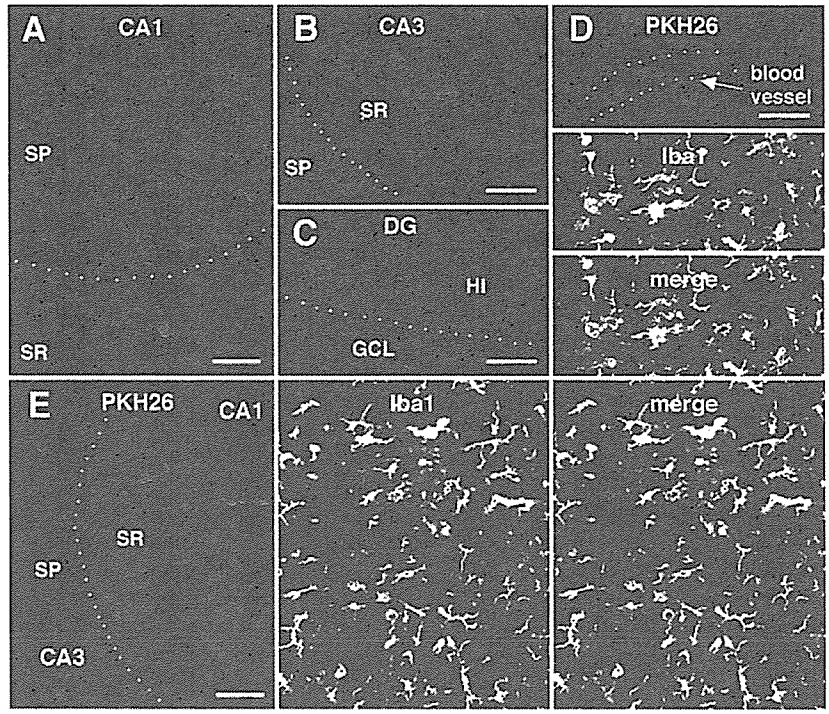

Fig. 1. Infiltration of arterial-injected PKH26-labeled microglia in the hippocampus at 24 after ischemia. (A–C) PKH26-labeled cells distributed in the CA1 subfield (A), the CA3 subfield (B), and the dentate hilus (C). (D, E) Immunofluorescent CLSM images for PKH26 (red) and Iba1 (green) in the CA3 subfield of the hippocampus. The hippocampal sections containing PKH-labeled cells were subjected to an indirect immunofluorescence analysis with anti-Iba1 antibody. Most PKH26-labeled cells were thus found to be positive for Iba1. Scale bars=50 μm (A–D), 80 μm (E).

RESULTS

Infiltration of intra-arterial injected microglia in the post-ischemic brain

In sham animals, PKH26-labeled cells were detected only in the vessels of the various brain regions but not in the brain parenchyma including the hippocampus. In the sections prepared from the animals subjected to the transient ischemia 24 h earlier, round- or oval-shaped PKH26-labeled cells were distributed throughout the hippocampus. In the CA1 subfield, PKH26-labeled cells were mainly detected in the pyramidal cell layer (Fig. 1A). On the other hand, in the CA3 subfield, PKH26-labeled cells were mainly distributed in the dendritic fields (Fig. 1B). PKH26-labeled cells were also scattered in the dentate hilus (Fig. 1C). The mean cell number of PKH26-labeled cells/section (10 μm thickness) in the CA1 and CA3 regions was 15.7±1.0 and 19.3±1.3 (number of sections=14), respectively. The total cell number of PKH26-labeled cells migrated in the hippocampus at 24 h after forebrain ischemia ranged from 1400–1800. When hippocampal sections were immunostained for Iba1, which is specifically expressed in cells of the monocytic lineage including microglia (Imai et al., 1996), PKH26-labeled cells adhered to the blood vessels were observed to be immunostained for Iba1 (Fig. 1D). Some cells resided in the parenchyma close to the blood vessels. As shown in Fig. 1E, most PKH26-labeled cells observed in the parenchyma were also positive for Iba1. In the sections prepared from the animals subjected to ischemia 48 h and 96 h earlier, however, PKH26-labeled cells were rarely detectable in the CA1 subfield.

Protective effects of intra-arterial microglial injection against the ischemia-induced changes in the evoked synaptic responses in the hippocampal CA1 pyramidal cells

Next, we examined the effects of the intra-arterial injection of microglia on the ischemia-induced changes in synaptic responses in hippocampal slices. The field potentials elicited by the stimulation of the CA3–CA1 Schaffer collateral pathway were simultaneously recorded from the somatic (upper traces) and dendritic (lower traces) areas of the hippocampal CA1 subfield prepared from the medium- and microglia-injected animals subjected to the transient ischemia.

In the sham slices of both groups, an upward waveform followed by a single population spike was recorded from the CA1 somatic area of sham slices. When recorded from the dendritic area of the CA1 subfield, the population excitatory postsynaptic potentials (pEPSPs) consisting of a downward waveform with a single positive reflection was observed. No significant difference in the synaptic responses was observed between these two groups (Fig. 2A, D). In the slices prepared from the medium-injected animals subjected to ischemia 48 h earlier, the mean max-

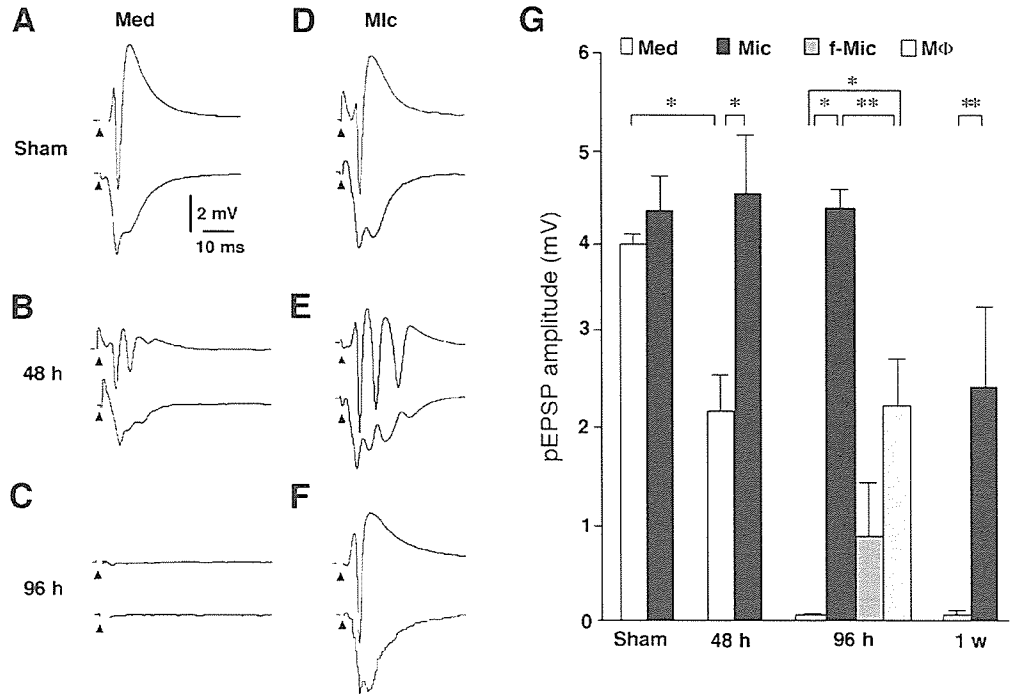

Fig. 2. Effects of the intra-arterial injection of microglia on the ischemia-induced changes of the synaptic field potentials in the hippocampal CA1 subfield. (A–C) Somatic (upper traces) and dendritic responses (lower traces) recorded simultaneously at various times after ischemia in the hippocampus prepared from medium (Med) -injected rats. (D–F) Somatic (upper traces) and dendritic responses (lower traces) recorded simultaneously at various times after ischemia in the hippocampus prepared from microglia (Mic) -injected rats. (A, D) Sham, (B, E) 48 h after ischemia, (C, F) 96 h after ischemia. These responses were evoked by the supra-maximal stimulation of Schaffer collateral afferents. The arrowheads indicate the onset of stimulation of the Schaffer collateral pathway. (G) The mean pEPSP amplitude in the CA1 subfield of hippocampal slices prepared from the Med-, Mic-, fixed-microglia- (f-Mic), or macrophage (Mϕ) -injected rats subjected to ischemia. Each column and vertical bar represents the mean and S.E. of 30 slices from five animals (Sam), 30 slices from five animals (48 h), 32 slices from five animals (96 h), 12 slices from three animals (1 w), 11 slices from three animals (f-Mic), 32 slices from five animals (Mϕ). Asterisks indicate a significant difference between the values (* $P<0.05$, ** $P<0.01$).

imal amplitude of pEPSP was significantly diminished compared with sham-operated control (Fig. 2B, G). In contrast, a pronounced hyperexcitability was observed in the hippocampal slices prepared from the microglia-injected animals at this stage. As shown in Fig. 2E, the synaptic field responses were characterized by multiple peaks. Furthermore, there was no significant change in the mean maximal amplitude of pEPSP recorded from the hippocampal slices subjected ischemia 48 h earlier as compared with sham-operated control (Fig. 2G). At 96 h after ischemia, no synaptic field potential was observed in the CA1 subfield of slices prepared from the medium-injected animals, while a presynaptic fiber volley was present (Fig. 2C). In the CA1 subfield of hippocampal slices prepared from the microglia-injected animals, rather normal responses were observed (Fig. 2F). In the microglia-injected animals, the synaptic field potentials of CA3–CA1 synapses were well preserved for up to 1 week (Fig. 2G). When the microglia fixed with 4% paraformaldehyde were injected intra-arterially, the pEPSP amplitude significantly decreased after ischemia (Fig. 2G). Intra-arterial injection of peripheral macrophages also showed a neuroprotective effect, while the mean restored amplitude of pEPSP of CA3–CA1 synapses by intra-arterial injection of microglia was on average 1.9-fold larger than that of intra-arterial injection of macrophage (Fig. 2G).

Protective effects of intra-arterial microglial injection against the ischemia-induced impairment of the efficacy of synaptic transmission

We have further examined the basal synaptic transmission and plasticity in the CA3–CA1 Schaffer collateral pathway of the medium- and microglia-injected animals subjected to ischemia 48 h earlier. We first constructed the input-output (I–O) relationships by plotting the mean pEPSP slope against the stimulus intensity. As shown in Fig. 3A, the mean pEPSP slope of the medium-injected animals stayed at a low level and it did not increase even after stronger stimulus intensities. On the other hand, no significant deficit in the I–O relationships was observed in the CA3–CA1 synapses of the microglia-injected animals (Fig. 3A). The mean maximal pEPSP slope of the microglia-injected animals was significantly larger than that of the medium-injected animals. Next, the I–O relationships were constructed by plotting the mean amplitude of the presynaptic fiber volley against the stimulus intensity. As shown in Fig. 3D, there was no significant difference between I–O curves of these two groups, thus indicating that the excitability of

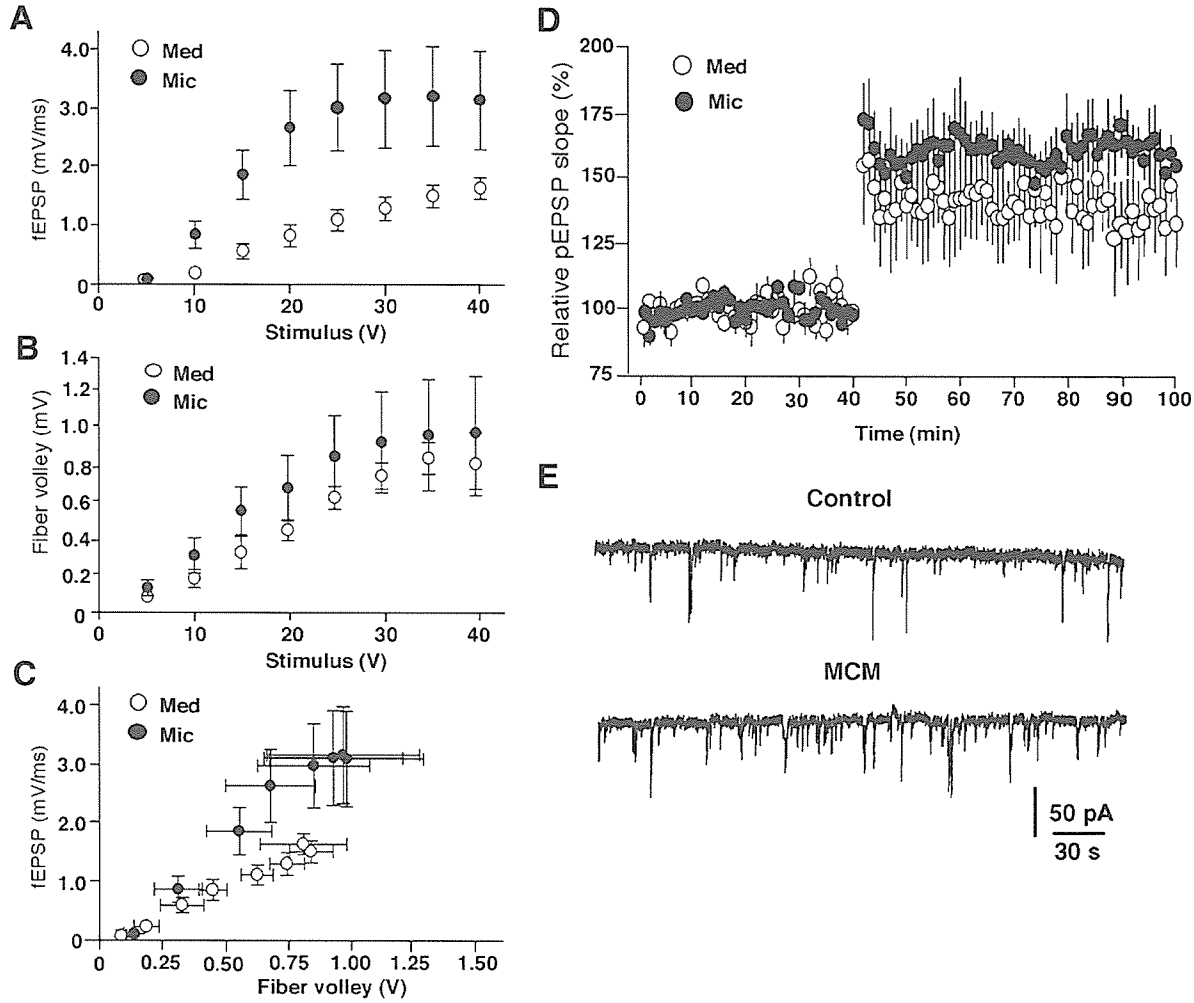

Fig. 3. (A–D) The effects of the intra-arterial injection of microglia on synaptic efficacy and LTP in the post-ischemic hippocampal CA1 subfield. (A–C) I–O relationships in the Schaffer collateral–CA1 synapses from the medium- (open circles) and microglia-injected animals (filled circles) subjected to ischemia 48 h earlier. (A) The mean pEPSP slope plotted against the stimulus intensity, (B) the mean amplitude of fiber volley plotted against the stimulus intensity, (C) the mean pEPSP slope plotted against the mean amplitude of fiber volley. (D) Relative pEPSP slope before and after tetanic stimulation (100 Hz, 1 s) in the CA3–CA1 synapses from the medium- and microglia-injected animals subjected to ischemia 48 h earlier. Each circle and bar represents mean and S.E. of three to five slices from three animals. (E) Effect of 10% MCM on spontaneous postsynaptic currents at a holding potential of −60 mV.

presynaptic fibers was not significantly affected by ischemia. When the I–O relationships were constructed by plotting the mean pEPSP slope against the mean amplitude of the presynaptic fiber volley, the mean slope of I–O curve of the microglia-injected rats (3.12±0.83 V/s, three slices from three animals) was significantly larger than that of the medium-injected rats (1.62±0.19 V/s, five slices from three animals) ($P<0.05$). Next, we also examined the formation of short-term synaptic plasticity and LTP in these two groups subjected to ischemia 48 h earlier. In both groups, there was no difference in paired-pulse facilitation between the medium- and microglia-injected animals (data not shown). As shown in Fig. 3D, the mean magnitude of LTP in the hippocampal slices prepared from the microglia-injected animals (159.4±7.7%, three slices from three animals) was larger than that from the medium-injected animals (136.4±13.5%, four slices from three animals). However, the difference did not reach statistical significance. These observations indicated that the ischemia-induced deficit in basal synaptic transmission and LTP in the CA3–CA1 synapses was markedly ameliorated by the arterial-injection of microglia.

To evaluate the possible effect of microglial diffusible factor(s) on presynaptic events, we further examined effects of MCM on spontaneous postsynaptic currents of CA1 neurons in hippocampal slices. As shown in Fig. 3E, the frequency of miniature response was significantly increased by 10% MCM. As shown in Fig. 3E, 10% MCM significantly increased the frequency of spontaneous postsynaptic currents by 130.5±15.4% of the control frequency ($P<0.05$, number of slices=4) without affecting the mean amplitude of the miniature responses. On the other hand, the 10% culture medium had no significant effect

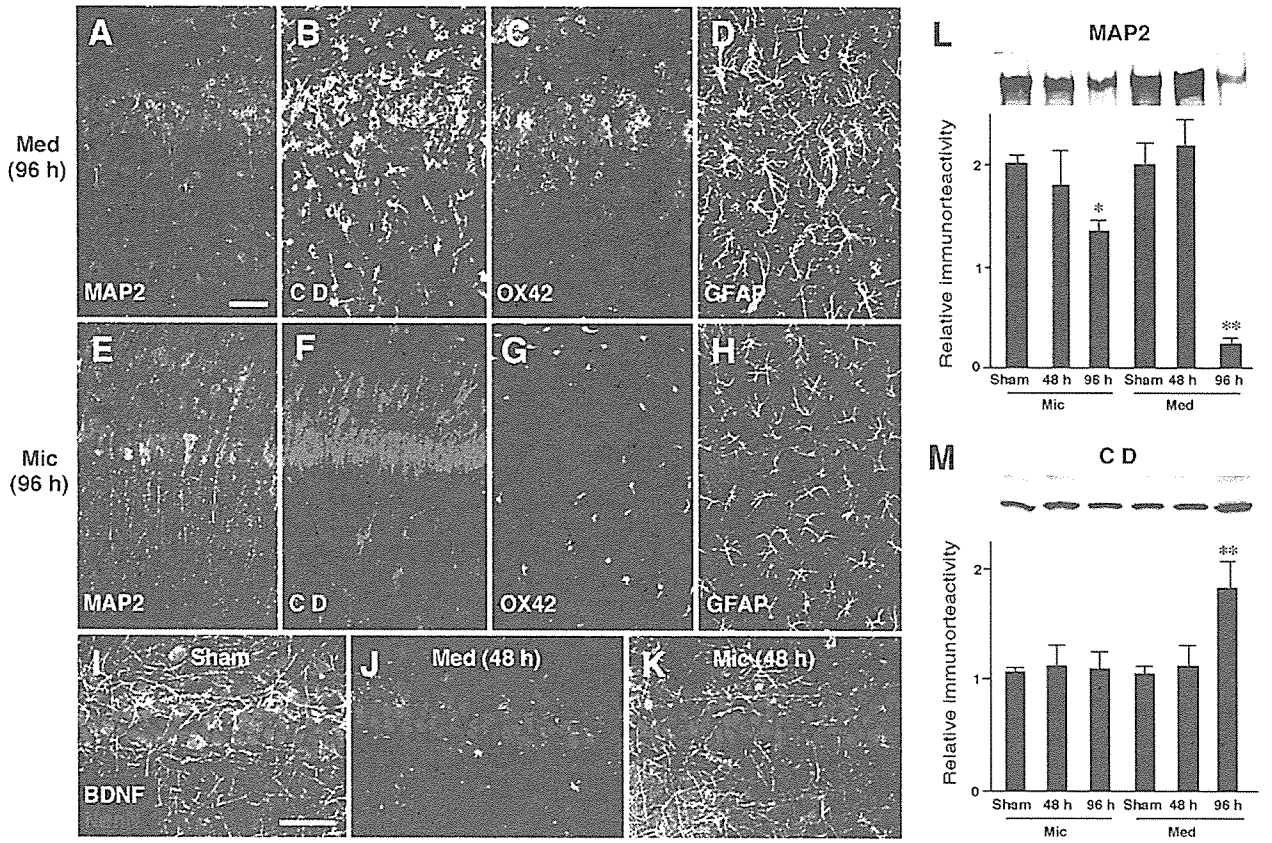

Fig. 4. Inhibition of ischemia-induced neurodegeneration and gliosis in the hippocampal CA1 subfield by the intra-arterial injection of microglia. (A–H) Immunofluorescent CLSM images (green) for MAP2 (A, E), CD (B, F), OX42 (C, G) and GFAP (D, H). (A–D) The hippocampus prepared from the medium (Med) -injected rats subjected to ischemia 96 h earlier. (E–H) The hippocampus prepared from the microglia (Mic) -injected rats subjected to ischemia 96 h earlier. The nuclei were stained by PI (red). Scale bar=100 μm. (I–K) Immunofluorescent double-labeled CLSM images for BDNF (green) and NeuN (red) in the hippocampal CA1 subfield. Sham: sham-operated rats, 48h (Med): Med-injected rat subjected to ischemia 48 h earlier, 48 h (Mic): Mic-injected rat subjected to ischemia 48 h earlier. Scale bar=50 μm. (L, M) Immunoblot analyses of the extracts of the hippocampus prepared from the Mic- and Med-injected rats subjected to ischemia by anti-MAP2 (L) or anti-CD antibody (M). Mic: hippocampal extracts prepared from the Mic-injected rats, Med: hippocampal extracts prepared from the Med-injected rats. Sham: sham-operated rats, 48 h: rat subjected to ischemia 48 h before, 96 h: rat subjected to ischemia 96 h before. Asterisks indicate a significant difference from the value obtained in the Sham rats (* $P<0.05$, ** $P<0.01$).

(97.3±4.2% of the control frequency, number of slices=4) (data not shown).

Effects of the intra-arterial microglial injection on the ischemia-induced neuronal death and gliosis in the hippocampal CA1 subfield

In the hippocampal sections prepared from the medium-injected animals subjected to ischemia 96 h earlier, marked neuronal degeneration and gliosis were obvious in the CA1 subfield as evidenced by condensed PI-stained nuclei of CA1 neurons and marked decrease in the immunoreactivity for MAP2 (Fig. 4A). It was also noted that the reduction of MAP2-immunorectivity was restricted in the CA1 subfield. Furthermore, GFAP and OX42-positive cells, which had thick processes, were frequently found in the CA1 subfield, indicating the formation of gliosis (Fig. 4C, D). The immunoreactivity for CD also markedly increased in the CA1 subfield (Fig. 4B). The increased immunoreactivity for CD is considered to mainly reflect gliosis due to neurodegeneration as previously reported (Nakanishi et al., 1993, 1994). Therefore, it is likely that the total loss of postsynaptic field potentials at this stage is due to an irreversible state of impairment. In contrast, we could not detect any significant loss of MAP2 immunoreactivity or a significant increase in CD immunoreactivity in the CA1 subfield of the hippocampal sections prepared from the microglia-injected animals subjected ischemia 96 h earlier (Fig. 4E, F). Furthermore, the signs for cellular activation of glial cells including morphological transformation and cell proliferation were barely detected in the CA1 subfield of these animals (Fig. 4G, H).

Immunohistological observations were further substantiated by immunoblot analyses. In the hippocampal extracts prepared from the medium-injected animals subjected to ischemia 96 h earlier, MAP2 level was significantly decreased (Fig. 4L). The mean amount of MAP2 was approximately 15% of that obtained from sham animals. In the hippocampal extracts prepared from the microglia-injected animals subjected to ischemia 96 h earlier, the level of MAP2 was markedly restored. The mean

amount of MAP2 was approximately 70% of that obtained from sham animals. On the other hand, the mean amount of CD significantly increased in the hippocampal extracts prepared from the medium-injected animals subjected to ischemia 96 h earlier (Fig. 4M). The increased immunoreactivity for CD is considered to mainly reflect gliosis due to neurodegeneration as reported previously (Nakanishi et al., 1993, 1994). In contrast, there was no significant change in the mean amount of CD in the postischemic hippocampus taken from the microglia-injected animals.

Finally, we examined the levels of BDNF immunoreactivity in the postischemic hippocampus taken from the medium- and microglia-injected animals subjected to ischemia, because the exogenously migrated microglia enhanced the BDNF level in neighboring neurons (Suzuki et al., 2001). In the sham animals, the intense immunoreactivities of BDNF were mainly found in the somata and dendrites of CA1 neurons (Fig. 4I). At 48 h after ischemia, the immunoreactivity of the BDNF in CA1 neurons of the medium-injected rats was markedly decreased (Fig. 4J). On the other hand, the immunoreactivity of BDNF in CA1 neuron of the microglia-injected animals remained well preserved (Fig. 4K). The mean level of intensity of BDNF immunofluorescence in the CA1 subfield of the ischemic hippocampus prepared from microglia-injected animals was on average 3.1-fold higher than from medium-injected animals (number of animals=3, $P<0.01$).

DISCUSSION

The major finding of the present study is that the intra-arterial injection of immortalized microglial cells, GMIR1, significantly ameliorated the ischemia-induced functional and morphological changes of hippocampal CA1 neurons in rats. In the hippocampal slices prepared from the medium-injected rats subjected to ischemia 48 h earlier, the evoked synaptic responses in the CA1 subfield became diminished without significant changes in levels of either MAP2 or CD. Our observations here are consistent with previous reports that the synaptic activity and plasticity both significantly decreased after ischemia (Urban et al., 1989; Hori and Carpenter, 1994; Kirino et al., 1992; Xu and Pulsinelli, 1994, 1996; Shinno et al., 1997). At 96 h after ischemia, the evoked synaptic responses in the CA1 subfield totally disappeared. At this stage, we found a significant decrease in the MAP2 level and a significant increase in the CD level in the hippocampus. Therefore, the decreased amplitude of evoked synaptic responses at 48 h after ischemia is most likely due to a dysfunction in the transmission rather than an irreversible state of impairment (Shinno et al., 1997; Zhang et al., 1999). On the other hand, the total loss of the postsynaptic field potentials at 96 h after ischemia is considered to reflect an irreversible state of impairment (Urban et al., 1989). In the present study, we found that the intra-arterial injection of microglia significantly protected the CA1 neurons against the ischemia-induced deficit in basal synaptic transmission and LTP in the CA3–CA1 glutamatergic synapses. The intra-arterial injection of microglia also inhibited the ischemia-induced neuronal degeneration and resultant gliosis in the CA1 subfield. The neuroprotective effect of intra-arterial-injected microglia was not observed by the fixation of microglia before injection. Therefore, the protective effect of intra-arterial-injected microglia on CA1 neurons against ischemic neuronal damage is considered to be due to the direct effect of infiltrated microglia rather than by indirect effects such as an incomplete reduction of the rCBF or hypothermia caused by the injection of microglia during occlusion. In the present study, approximately 2000 cells of exogenous microglia were found to migrate to the hippocampus after intra-arterial injection of 2×10^6 cells. This is consistent with the observations reported by Kitamura et al. (2004) that neuroprotective effect of i.c.v.-injected 4000 cells of microglia was equal to or may be higher than that of the 40,000 cells of microglia. Therefore, it is reasonable to consider that approximately 2000 of the microglial cells at the pathological site were sufficient to exert neuroprotection against ischemic neuronal damage.

Transient forebrain ischemia causes a complex cellular response that leads to the delayed neuronal death of specific neuronal populations in both humans and animal models (Pulsinelli et al., 1982; Kirino, 1982; Zola-Morgan et al., 1986, 1992). Even though extensive studies have been performed, the delayed nature of neuronal death of hippocampal CA1 neurons is still not fully understood. Shinno et al. (1997) have demonstrated that the reduction of the synaptic transmission in CA1 neurons in the early phase of ischemic insult may cause disruption of neurotrophic supply, thus leading to the apoptotic process. There is accumulating evidence that the ischemia-induced synaptic dysfunction may result from a low probability of transmitter release. Zhang et al. (1999) have reported that the amplitude of population spikes evoked in the CA1 subfield of hippocampal slices prepared from the post-ischemic rats was significantly restored by 4-aminopyridine, which is known to enhance transmitter release probability. More recently, it has been reported that ischemia-like condition (anoxia and aglycemia) significantly reduced the mean frequency of miniature excitatory postsynaptic currents recorded from CA1 neurons without affecting the amplitude (Tanaka et al., 2001). It has been recognized that the neuronal activity and neurotrophic factors interact reciprocally. The blockade of synaptic activities with TTX inhibits production and release of BDNF (Castrén et al., 1992), whereas glutamate stimulates BDNF production and release (Zafra et al., 1991). Furthermore, both mRNA and protein levels of BDNF were significantly decreased in the hippocampus after ischemia (Kokaia et al., 1996; Lee et al., 2002). Our observations herein showed that the intra-arterial injection of microglia prevented the ischemia-induced reduction of the BDNF levels in CA1 neurons. In the present study, we also found that MCM significantly increased the frequency of spontaneous postsynaptic currents of CA1 neurons without affecting the amplitude, thus indicating that MCM increased the provability of the neurotransmitter release. Therefore, it is tempting to speculate that the exogenously migrated microglia in the hippocampus ameliorated the ischemia-induced synaptic hypoactiv-

ity by the release of diffusible factor(s) that may increase the release of glutamate. The intra-arterial injection of microglia then preserved the BDNF levels, thus protecting CA1 neurons against the ischemia-induced neuronal degeneration. Furthermore, we recently reported that microglia secrete soluble factors that facilitate *N*-methyl-D-aspartic acid (NMDA) receptor-mediated glutamatergic neurotransmission (Moriguchi et al., 2003; Hayashi et al., 2006). These diffusible factors released by the exogenously migrated microglia may also contribute to the increased expression of BDNF because the activation of synaptic NMDA receptors has been shown to increase the expression level of BDNF (Hardingham et al., 2002). Additional experiments are necessary to identify the microglial diffusible factor(s) that could ameliorate the ischemia-induced synaptic deficits.

CONCLUSION

In conclusion, the arterial-injection of microglia protected against the ischemia-induced neuronal degeneration in the hippocampus possibly through the restoration of basal glutamatergic transmission and BDNF levels. Therefore, the arterial-injection of microglia might thus be a potentially effective therapeutic modality for the treatment of acute brain injury including cerebral ischemia.

Acknowledgments—This study was supported by Grants-in-Aid for the Creation of Innovations through Business-Academic-Public Sector Cooperation of Japan, and Grants-in-Aid for Scientific Research on Priority Area (No.15082204) from the Ministry of Education, Science and Culture, Japan.

REFERENCES

Castrén E, Zafra F, Thoenen H, Lindholm D (1992) Light regulates expression of brain-derived neurotrophic factor mRNA in rat visual cortex. Proc Natl Acad Sci U S A 89:9444–9448.

Hardingham GE, Fukunaga Y, Bading H (2002) Extrasynaptic NMDARs oppose synaptic NMDARs by triggering CREB shut-off and cell death pathways. Nat Neurosci 5:405–414.

Hayashi Y, Ishibashi H, Hashimoto K, Nakanishi H (2006) Potentiation of the NMDA receptor-mediated responses through the activation of the glycine site by microglia secreting soluble factors. Glia 53:660–668.

Hori N, Carpenter DO (1994) Functional and morphological changes induced by transient in vivo ischemia. Exp Neurol 129:279–289.

Imai F, Sawada M, Suzuki H, Kiya N, Hayakawa M, Nagatsu T, Marunouchi T, Kanno T (1997) Migration activity of microglia and macrophages into rat brain. Neurosci Lett 237:49–52.

Imai F, Sawada M, Suzuki H, Zlokovic BV, Kojima J, Kuno S, Nagatsu T, Nitatori T, Uchiyama Y, Kanno T (1999) Exogenous microglia enter the brain and migrate into ischaemic hippocampal lesions. Neurosci Lett 272:127–130.

Imai Y, Ibata I, Ito D, Ohsawa K, Kohsaka S (1996) A novel gene iba1 in the major histocompatibility complex class III region encoding an EF hand protein expressed in a monocytic lineage. Biophys Biochem Res Commun 224:855–862.

Kirino T (1982) Delayed neuronal death in the gerbil hippocampus following ischemia. Brain Res 239:57–69.

Kirino T, Robinson HPC, Miwa A, Tamura A, Kawai N (1992) Disturbance of membrane function preceding ischemic delayed neuronal death in the gerbil hippocampus. J Cereb Blood Flow Metab 12:408–417.

Kitamura Y, Takata K, Inden M, Tsuchiya D, Yanagisawa D, Nakata J, Taniguchi T (2004) Intraventricular injection of microglia protects against focal brain ischemia. J Pharmacol Sci 94:203–206.

Kitamura Y, Yanagisawa D, Inden M, Takata K, Tsuchiya D, Kawasaki T, Taniguchi T, Shimohama S (2005) Recovery of focal brain ischemia-induced behavioral dysfunction by intracerebroventricular injection of microglia. J Pharmacol Sci 97:289–293.

Kokaia Z, Nawa H, Uchino H, Elmér E, Kokaia M, Carnahan J, Smith ML, Siesjö BK, Lindvall O (1996) Regional brain-derived neurotrophic factor mRNA and protein levels following transient forebrain ischemia in the rat. Mol Brain Res 38:139–144.

Lee TH, Kato H, Chen ST, Kogre K, Itoyama Y (2002) Expression disparity of brain-derived neurotrophic factor immunoreactivity and mRNA in ischemic hippocampal neurons. Neuroreport 13: 2271–2275.

Lees GJ (1993) The possible contribution of microglia and macrophages to delayed neuronal death after ischemia. J Neurol Sci 114:119–122.

Liu J, Bartels M, Lu A, Sharp FR (2001) Microglia/macrophages proliferate in striatum and neocortex but not in hippocampus after brief global ischemia that produces ischemic tolerance in gerbil brain. J Cereb Blood Flow Metab 21:361–373.

Moriguchi S, Mizoguchi Y, Tomimatsu Y, Hayashi Y, Kadowaki T, Kagamiishi Y, Katsube N, Yamamoto K, Inoue K, Watanabe S, Nabekura J, Nakanishi H (2003) Potentiation of NMDA receptor-mediated synaptic responses by microglia. Mol Brain Res 119: 160–169.

Morihata H, Kawasaki J, Sakai H, Sawada M, Tsutada T, Kuno M (2000) Temporal fluctuations of voltage-gated proton currents in rat spinal microglia via pH- dependent and -independent mechanisms. Neurosci Res 38:265–271.

Nakanishi H, Tsukuba T, Kondou T, Tanaka T, Yamamoto K (1993) Transient forebrain ischemia induces expression and specific localization of cathepsins E and D in rat hippocampus and neostriatum. Exp Neurol 121:215–223.

Nakanishi H, Tominaga K, Amano T, Yamamoto K (1994) Age-related changes in activities and localizations of cathepsins D, E, B and L in the rat brain tissues. Exp Neurol 126:119–128.

Pulsinelli WA, Brierley JB (1979) A new model of bilateral hemispheric ischemia in the unanesthetized rat. Stroke 10:267–272.

Pulsinelli WA, Brierley JB, Plum F (1982) Temporal profile of neuronal damage in a model of transient forebrain ischemia. Ann Neurol 11:491–498.

Salimi K, Moser K, Zassler B, Reindl M, Embacher N, Schermer C, Wes C, Marksteiner J, Sawada M, Humpel C (2002) Glial cell line-derived neurotrophic factor enhances survival of GM-CSF dependent rat GMIR1-microglial cells. Neurosci Res 43:221–229.

Sawada M, Imai F, Suzuki H, Hayakawa M, Kanno T, Nagatsu T (1998) Brain-specific gene expression by immortalized microglial cell-mediated gene transfer in the mammalian brain. FEBS Lett 433:37–40.

Shimizu T, Hayashi Y, Yamasaki R, Yamada J, Zhang J, Ukai K, Koike M, Mine K, von Figura K, Peters C, Saftig P, Fukuda T, Uchiyama Y, Nakanishi H (2005) Proteolytic degradation of glutamate decarboxylase mediates disinhibition of hippocampal CA3 pyramidal cells in cathepsin D-deficient mice. J Neurochem 94:680–690.

Shinno K, Zhang L, Eubanka JH, Carlen PL, Wallance MC (1997) Transient ischemia induces an early decrease of synaptic transmission in CA1 neurons of rat hippocampus: electrophysiologic study in brain slices. J Cereb Blood Flow Metab 17:955–966.

Suzuki H, Imai F, Kanno T, Sawada M (2001) Preservation of neurotrophin expression in microglia that migrate into the gerbil's brain across the blood-brain barrier. Neurosci Lett 312:95–98.

Tanaka E, Yasumoto S, Hattori G, Niyama S, Matsuyama S, Higashi H (2001) Mechanism underlying the depression of evoked fast EPSCs following in vitro ischemia in rat hippocampal CA1 neurons. J Neurophysiol 86:1095–1103.

Tomimatsu Y, Idemoto K, Moriguchi S, Watanabe S, Nakanishi H (2002) Proteases involved in long-term potentiation. Life Sci 72:355–361.

Urban L, Neill KH, Crain BJ, Nadler JV, Somjen GG (1989) Postischemic synaptic physiology in area CA1 of the gerbil hippocampus studied in vitro. J Neurosci 9:3966–3975.

Xu ZC, Pulsinelli WA (1994) Responses of CA1 pyramidal neurons in rat hippocampus to transient forebrain ischemia: an in vivo intracellular recording study. Neurosci Lett 171:187–191.

Xu ZC, Pulsinelli WA (1996) Electrophysiological changes of CA1 pyramidal neurons following transient forebrain ischemia: an in vivo intracellular recording and staining study. J Neurophysiol 76: 1689–1697.

Yrjänheikki J, Keinänen R, Pellikka M, Hökfelt T, Koistinaho J (1998) Tetracyclines inhibit microglial activation and are neuroprotective in global brain ischemia. Proc Natl Acad Sci U S A 95:15769–15774.

Zafra F, Castrén E, Thoenen H, Lindholm D (1991) Interplay between glutamate and γ-aminobutyric acid transmitter systems in the physiological regulation of brain-derived neurotrophic factor and nerve growth factor synthesis in hippocampal neurons. Proc Natl Acad Sci U S A 88:10037–10041.

Zhang L, Shang Y, Tian GF, Wallance MC, Eubanks JH (1999) Reversible attenuation of glutamatergic transmission in hippocampal CA1 neurons of rat brain slices following transient cerebral ischemia. Brain Res 832:31–39.

Zola-Morgan S, Squire LR, Amaral DG (1986) Human amnesia and the media temporal region: enduring memory impairment following a bilateral lesion limited to field of the hippocampus. J Neurosci 6:1967–2950.

Zola-Morgan S, Squire LR, Rempel NL, Clower PR, Amaral DG (1992) Enduring memory impairment in monkeys after ischemic damage to the hippocampus. J Neurosci 12:2582–2596.

(Accepted 2 June 2006)
(Available online 14 July 2006)

Available online at www.sciencedirect.com
ScienceDirect
Biochemical and Biophysical Research Communications 349 (2006) 913–919
BBRC
www.elsevier.com/locate/ybbrc

Cell cycle-dependent regulation of kainate-induced inward currents in microglia

Jun Yamada [a], Makoto Sawada [b], Hiroshi Nakanishi [a,*]

[a] *Laboratory of Oral Aging Science, Faculty of Dental Sciences, Kyushu University, Fukuoka 812-8582, Japan*
[b] *Department of Brain Life Science, Research Institute of Environmental Medicine, Nagoya University, Nagoya 464-8601, Japan*

Received 8 August 2006
Available online 31 August 2006

Abstract

Microglia are reported to have α-amino-hydroxy-5-methyl-isoxazole-4-propionate/kainate (KA) types. However, only small population of primary cultured rat microglia (approximately 20%) responded to KA. In the present study, we have attempted to elucidate the regulatory mechanism of responsiveness to KA in GMIR1 rat microglial cell line. When the GMIR1 cells were plated at a low density in the presence of granulocyte macrophage colony-stimulating factor, the proliferation rate increased and reached the peak after 2 days in culture and then gradually decreased because of density-dependent inhibition. At cell proliferation stage, approximately 80% of the GMIR1 cells exhibited glutamate (Glu)- and KA-induced inward currents at cell proliferation stage, whereas only 22.5% of the cells showed responsiveness to Glu and KA at cell quiescent stage. Furthermore, the mean amplitudes of inward currents induced by Glu and KA at cell proliferation stage (13.8 ± 3.0 and 8.4 ± 0.6 pA) were significantly larger than those obtained at cell quiescent stage (4.7 ± 0.8 and 6.2 ± 1.2 pA). In the GMIR1 cells, KA-induced inward currents were markedly inhibited by (*RS*)-3-(2-carboxybenzyl) willardiine (UBP296), a selective antagonist for KA receptors. The KA-responsive cells also responded to (*RS*)-2-amino-3-(3-hydroxy-5-*tert*-butylisoxazol-4-yl) propanoic acid (ATPA), a selective agonist for GluR5, in both GMIR1 cells and primary cultured rat microglia. Furthermore, mRNA levels of the KA receptor subunits, GluR5 and GluR6, at the cell proliferation stage were significantly higher than those at the cell quiescent stage. Furthermore, the immunoreactivity for GluR6/7 was found to increase in activated microglia in the post-ischemic hippocampus. These results strongly suggest that microglia have functional KA receptors mainly consisting of GluR5 and GluR6, and the expression levels of these subunits are closely regulated by the cell cycle mechanism.

Keywords: Microglia; Kainate; Granulocyte–macrophage colony-stimulating factor; Whole-cell patch clamp; Real-time quantitative RT-PCR

There is increasing evidence that glutamate (Glu) is one of the important molecules mediating the neuron-to-microglia communication in both physiological and pathological states [1–5]. We have previously reported that microglia express functional ionotropic Glu receptors, mainly α-amino-hydroxy-5-methyl-isoxazole-4-propionate (AMPA)/kainate (KA) types. Although the activation of these receptors enhanced the release of proinflammatory cytokines including tumor necrosis factor-α, only 20% of the primary cultured rat microglia could elicit inward currents after the application of KA [5]. However, the reason why the KA-responsive population of the microglia is so small. Gottlieb and Matute [6] have reported that the levels of Glu receptor subunits expressed in the microglia peaked between 3 and 7 days after transient forebrain ischemia, a time when strong microglial activation and proliferation were observed in the CA1 subfield of the hippocampus [7]. Furthermore, it is also known that a marked expression of cyclin D1, a key regulator of cell cycle progression, was followed by microglial proliferation [7,8]. This may suggest that the expression of Glu receptors in the microglia is closely linked with the cell cycle. To investigate this

* Corresponding author. Fax: +81 92 642 6415.
E-mail address: nakan@dent.kyushu-u.ac.jp (H. Nakanishi).

0006-291X/$ - see front matter © 2006 Elsevier Inc. All rights reserved.
doi:10.1016/j.bbrc.2006.08.126

possibility, we examined the responses of the microglia to KA at different stages of cellular proliferation using the GMIR1 rat microglial cell line, which proliferates in response to granulocyte–macrophage colony-stimulating factor (GM-CSF) [9]. In the present study, we therefore provide evidence that a cell cycle-dependent regulation of both the response to KA and the expression level of KA receptor subunits exist in the microglia.

Materials and methods

Cell culture. GMIR1, an immortalized microglial clone, was established from a rat primary culture using a nonenzymatic and non-virus-transformed procedure [9,10]. The medium to maintain the GMIR1 cells was Eagle's minimal essential medium (MEM) supplemented with 10% fetal bovine serum (FBS) (Wako Pure Chemical Industries, Ins., Osaka, Japan), 5 μg/ml insulin, 0.17% $NaHCO_3$, 0.2% glucose, 2 mM glutamine, 100 U/ml penicillin, and 0.1 mg/ml streptomycin. 0.2 ng/ml rat recombinant GM-CSF (Genzyme, Cambridge, MA, USA) was supplemented in the culture medium to maintain the GMIR1 cells because these cells stop proliferating without it. The GMIR1 cells were grown in an atmosphere of 10% CO_2 at 37 °C and the medium was changed every 2–3 days. Every 2 months, new cells were started to avoid transformation. Primary cultured rat microglia were isolated from mixed glial cell cultures from the cerebral cortex of 3-day-old Wistar rats on the 14 day as reported previously [11]. Cultures were maintained in Eagle's MEM containing 10% FBS, 0.2% $NaHCO_3$, 2 mM glutamine, 0.2% glucose, 25 μg/ml insulin, 5000 U/ml penicillin, and 5 mg/ml streptomycin.

Electrophysiology. Whole-cell recordings were made as reported previously [2,5]. Microglial cells were whole-cell clamped using a patch pipette containing (in mM): CsCl 100, Na_2ATP 3, HEPES 5, $CaCl_2$ 1, $MgCl_2$ 4, EGTA 5, and *N*-methyl-D-glucamine (NMDG) 10. The pH of the solution was adjusted to 7.2 with NMDG. The pipette resistance was 5–8 MΩ. The external solution contained (in mM): KCl 2.5, NaCl 110, $CaCl_2$ 3, $BaCl_2$ 6, glucose 15, and HEPES 5, and the pH were adjusted to 7.4 with NMDG. Patch clamp recordings were obtained using an Axopatch 200B amplifier (Axon Instruments, Foster City, CA, USA) in voltage clamp mode. Na^+ free solutions were substituted NaCl for NMDG. The external KA or drugs were applied rapidly using the Y tube technique, which allows for the complete exchange of the external solution surrounding a cell within 20 ms. pH of KA solution was adjusted to 7.4 with 1 N NaOH. The experiments were performed at room temperature. Many GMIR1 cells showed a small round shape under phase-contrast microscopy. We recorded small rounded cells for electrophysiological recordings. KA, Glu, and (*RS*)-2-amino-3-(3-hydroxy-5-*tert*-butylisoxazol-4-yl) propanoic acid (ATPA) were purchased from Sigma (St. Louis, MO, USA). (*RS*)-3-(2-carboxybenzyl) willardiine (UBP296) was purchased from Wako Pure Chemical Industries.

BrdU incorporation. The GMIR1 cells were plated 10^4 per one cover glass coated with polyethyllenimine and then stained with a BrdU immunohistochemistry kit (EMD Biosciences, Inc., La Jolla, CA, USA) according to the manufacturer's protocol. The images were obtained with a microscope (Akisionscope, Carl Zeiss) using a 40× water immersion objective. Images were transferred to a personal computer and analyzed using the Image J software program (v 3.04). A statistical analysis was carried out using ANOVA. A value of $P < 0.05$ was considered to indicate statistical significance.

Real-time quantitative RT-PCR. Total RNAs were prepared from 2 to 2.5×10^6 cells with a RNeasy RNA purification kit (Qiagen, Hilden, Germany). To avoid any contamination of genomic DNA, cytoplasmic RNAs were isolated and DNase was added according to the manufacturer's protocol. RT minus controls were run to confirm the presence of genomic contamination. First strand cDNA synthesized from 1 mg of total RNA with random hexamer primers and oligo (dT) primers was used as template in each reaction. Syber green based real-time RT-PCR was performed with DyNAmo SYBER Green 2-step qRT-PCR kit (Finnzymes, Espoo, Finland). Rotor Gene 3000 (Corbett Research, Mortlake, Australia) was used for the signal detection. PCR was performed using 1× master mix, 0.5 μM of each primer. For standardization, rat GAPDH was used. The primers for detection of cyclin D1, GluR5–7, and KA1-2 cDNAs were as follows: cyclin D1 (232 bp), 5′-GCGTACCCTGACACCAATCT-3′ and 5′-GCTCCAGAGACAA GAAACGG-3′; GluR5 (208 bp), 5′-GCCCCTCTCACCATCACAT AC-3′ and 5′-ACCTCGCAATCACAAACAGTACA-3′; GluR6 (260 bp) 5′-TTCCTGAATCCTCTCTCCCCT-3′ and 5′-CACCAAATGCCTCC CACTATC-3′; GluR7 (423 bp) were 5′-TGGGCCTTCACCTTGAT CATCA-3′ and 5′-ACTCCACACCCCGACCTTCT-3′; KA1 (267 bp), 5′-GGATCGCTGCTATCTTGGATG-3′ and 5′-CCTTCTCTCCACA GATGTTGCT-3′; KA2 (291 bp), 5′-ACAGCCAGTACGAGACTAC-3′ and 5′-ACTCAGC TTTGGCGCAGAT-3′. PCR conditions were 95 °C for 15 min, followed by 35–40 cycles at 94 °C for 10 s, 49–56 °C for 20 s, and 72 °C for 20 s. After real-time RT-PCR, the reaction products were analyzed by electrophoresis on ethidium bromide, stained agarose gel. All of the PCR experiments were performed in duplicate to verify the results.

Transient forebrain ischemia. Male Wistar rats (8 weeks) were subjected to transient forebrain ischemia by clamping the carotid arteries bilaterally as reported previously [12,13]. Briefly, the animals were anesthetized with a mixture of ketamine (50 mg/kg) and xylazine (10 mg/kg), and bilateral vertebral arteries were electrocauterized at the level of the first vertebra. On the following day, the common carotid arteries were gently exposed and both arteries were occluded with a vascular clamp for 15 min. The rectal temperature was maintained at 36.5–37.5 °C. Rats that had lost their righting reflexes during the period of ischemia were used as the postischemic group.

Immunohistochemistry. Animals were anesthetized with sodium pentobarbital (40 mg/kg, i.p.) and killed by intracardiac perfusion with isotonic saline followed by a chilled fixative consisting of 4% paraformaldehyde in 0.1 M PB (pH 7.4). After perfusion, the brain was removed and further fixed by immersion in the same fixative overnight at 4 °C, and then immersed in 30% sucrose (pH 7.4) for 72 h at 4 °C. Floating parasagittal sections (30 μm thick) of the hippocampus were prepared by a cryostat (CM1850, Leica, Nussloch, Germany). After blocking with 10% normal goat serum overnight at 4 °C, they were stained with anti-GluR6/7 (10 μg/ml) (Upstate, Lake Placid, NY, USA), anti-CD11b (1: 100) (OX42, Serotec, Bichester, UK) for 3 days at 4 °C. After washing with phosphate-buffered saline (PBS), sections were stained with goat anti-rabbit IgG-conjugated Alexa488 (Jackson Immunoresearch, West Grove, PA, USA) or goat anti-mouse IgG-conjugated Cy3 (Jackson Immunoresearch) for 6 h at 4 °C. The sections were mounted in the anti-fading medium Vectashield (Vector Laboratories, Burlingame, CA, USA) and examined by a confocal laser scanning microscope (CLSM) (LSM510MET, Carl Zeiss, Jena, Germany).

Statistics. The significance of the differences was examined by Student's *t*-test, using Kaleida Graph 3.6 J, and $P < 0.05$ was considered significant.

Results

Density-dependent inhibition of GM-CSF-induced cell proliferation of the GMIR1 cells

Most GMIR1 cells showed an ameboid-like morphology. When the GMIR1 cells were plated at a low cell density in the presence of 0.2 ng/ml GM-CSF, the number of cells markedly increased and reached a confluent state after 7 days in culture (Fig. 1A). The cellular proliferation of the GMIR1 cells was fully dependent on GM-CSF and the number of cells did not change without GM-CSF. The total number of cells increased by approximately 260%, 400%, and 500% after 2, 5, and 7 days in culture, respectively. On the other hand, the ratio of BrdU-incorpo-

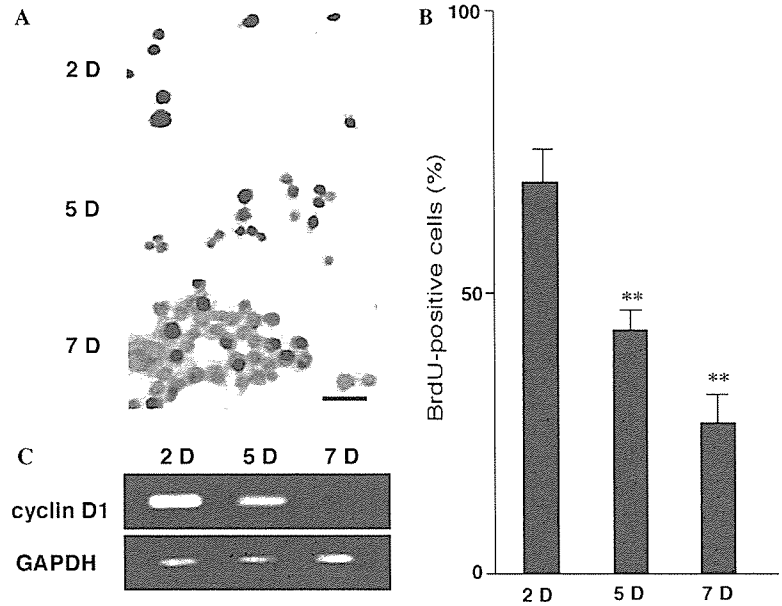

Fig. 1. Density-dependent inhibition of the proliferation of a microglia cell line, GMIR1. (A) BrdU incorporation into the GMIR1 cells after 2 (2D), 5 (5D), and 7 (7D) days in culture with the cell density of 1×10^4 cells/well. Scale bar, 15 μm. (B) The ratio of BrdU-positive cells to total cells at 2D, 5D, and 7D. Each column and vertical bar represents the mean and SE of four experiments, respectively. Asterisks indicate a significant difference from 2D (**$P < 0.01$, Student's t-test). (C) The expression of cyclin D1 mRNA in the GMIR1 cells at 2D, 5D, and 7D.

rated cells reached a peak after 2 days in culture and then gradually decreased (Fig. 1A and B). We next examined the expression of cyclin D1 in the GMIR1 cells. Relatively high expression levels of mRNA encoding cyclin D1 were seen in the GMIR1 cells after 2 days in culture (Fig. 1C). After 7 days in culture, the specific band of cyclin D1 could not be found. These observations indicate that the GMIR1 cells exhibited a cell density-dependent inhibition of proliferation in the presence of GM-CSF. Most cells proliferated after 2 days in culture, while most cells stopped cell division after 7 days in culture.

Cell cycle-dependent inhibition of responses for Glu and KA in the GMIR1 cells

We next examined effects of the cell cycle on the responses to Glu and KA in the GMIR1 cells. The application of Glu and KA induced inward currents under voltage clamp conditions at a holding potential of −60 mV. After 2 days in culture, 20 out of 25 cells (80%) exhibited relatively large inward currents after treatment with Glu and KA (Fig. 2A). The mean amplitudes of inward currents evoked by Glu and KA after 2 days in culture were 13.8 ± 3.0 and 8.4 ± 0.6 pA, respectively. After 5 days in culture, 7 out of 15 cells (46.7%) showed moderate responses to Glu and KA. After 7 days in culture, 18 out of 80 cells (22.5%) showed only small responses to Glu and KA. The mean amplitudes of inward currents evoked by Glu and KA after 7 days in culture were 4.7 ± 0.8 and 6.2 ± 1.2 pA, respectively. As shown in Fig. 2B, the mean normalized responses to Glu and KA in the GMIR1 cells after 7 days in culture were significantly smaller that those in GMIR1 cells after 2 days in culture. We also examined the effects of cell cycle on the responses to ATP in the GMIR1 cells. In contrast to the responses to Glu and KA, all cells exhibited large inward currents even after 7 days in culture and cell cycle-dependent inhibition of responses was not observed.

The KA-induced currents were concentration dependent between 10^{-5} M and 3×10^{-3} M (data not shown). The mean amplitudes of the inward currents induced by each concentration of KA between 10^{-5} M and 3×10^{-3} M were normalized to the one induced by 3×10^{-3} M KA in the same cell. The concentration–response relationship in the GMIR1 cells after 2 days in culture showed that the half-activation concentration, and the Hill coefficients were 6.8×10^{-5} M and 1.3, respectively. We further examined effects of a specific antagonist and agonist for KA receptors. In the GMIR1 cells after 2 days in culture, the KA-induced (100 μM) inward currents were markedly inhibited by UBP296 (30 μM), a selective antagonist for KA receptors [14] (Fig. 3A). The similar results with the GMIR1 cells in quiescent stage were obtained in the primary cultured rat microglia that do not increase in cell number in the absence of mitogens. In the primary cultured rat microglia, KA induced inward currents in 3 out of 35 cells examined (8.6%). In these KA-responsive cells, ATPA also induced inward currents (Fig. 3B). Furthermore, ATPA (30 μM), a selective agonist for GluR5 [15], induced inward currents in the GMIR1 cells. When extracellular Na^+ was replaced with NMDG, the ATPA-induced inward currents markedly decreased (Fig. 3C). On the other hand, the ATP-induced inward currents were not affected by the Na^+-free condition (Fig. 3C).

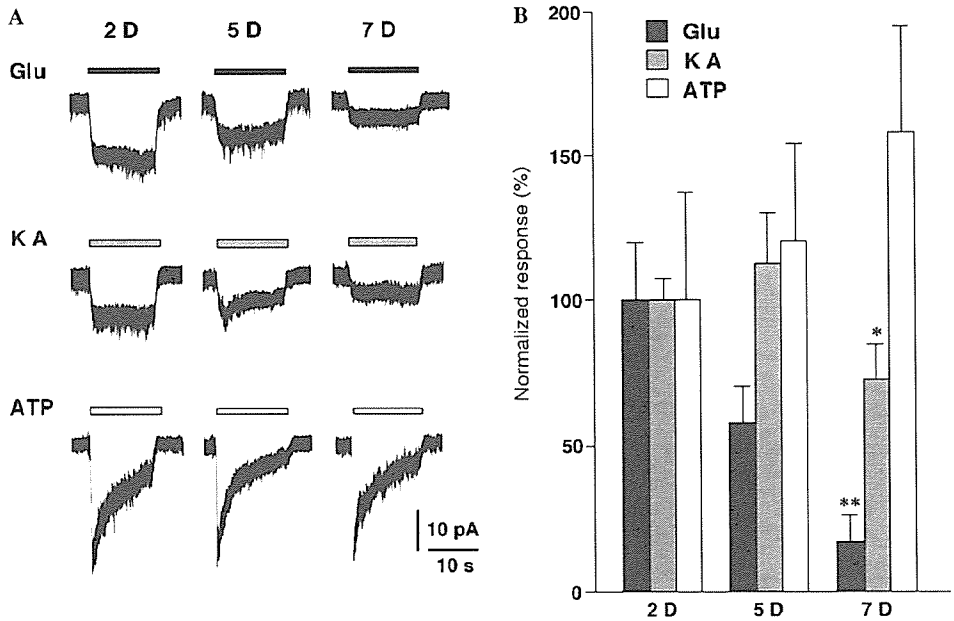

Fig. 2. Density-dependent reduction of the amplitude of the KA-induced inward currents in the GMIR1 cells. (A) KA (100 μM), Glu (100 μM), and ATP (100 μM)-induced inward currents in the GMIR1 cells at 2D, 5D, and 7D. The holding potential was −60 mV. (B) The mean normalized responses to Glu, KA, and ATP at 2D, 5D, and 7D. Each column and vertical bar represents the mean and SE of 7–15 experiments, respectively. Asterisks indicate a significant difference from 2D ($^{*}P < 0.05$, $^{**}P < 0.01$, Student's t-test).

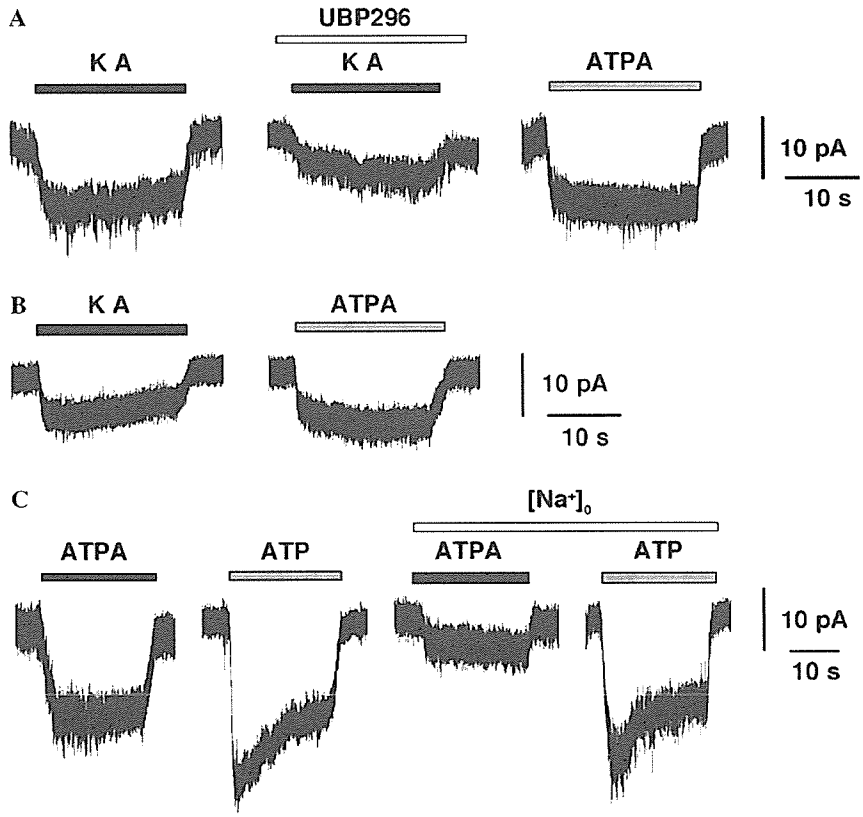

Fig. 3. The expression of functional KA receptors in the GMIR1 cell. (A) The inhibition of KA-induced inwards currents by 30 μM UBP296, a selective antagonist of KA receptor GluR5. ATPA (30 μM), a GluR5 selective agonist, also induced inward currents. (B) KA- and ATPA-induced inward currents in primary cultured rat microglia. (C) The effects of Na^{+}-free solution on the ATPA- and ATP-induced inward currents. When the external solution was replaced with Na^{+}-free ($[Na^{+}]_0$) solution, the amplitude of the ATPA-induced inward currents was markedly reduced.

Density-dependent downregulation of the expression levels of GluR5 and GluR6 in the GMIR1 cells

KA receptors are composed of five different subunits, namely GluR5, GluR6, GluR7, KA1, and KA2. GluR5, GluR6, and GluR7 assemble to form functional ion channels, whereas little is known about the functions of KA1 and KA2 [16]. Real-time quantitative RT-PCR was performed to examine the possible cell cycle-dependent alteration of KA receptor subunits, GluR5, GluR6, GluR7, KA1, and KA2. Our RT-PCR study showed that microglia expressed GluR5, GluR6, and KA2 mRNA, while GluR7 and KA1 mRNA were not detected (Fig. 4A). In comparison to the expression levels after 2 days in culture, the expression level of GluR5 mRNA significantly declined to 70.6 ± 17.0% and 47.8 ± 16.0% after 5 and 7 days in culture, respectively (Fig. 4B). Furthermore, the GluR6 mRNA expression levels also decreased to 41.2 ± 2.0% and 17.3 ± 1.9% after 5 and 7 days in culture, respectively. The expression levels of KA2 mRNA did not show any significant change. These observations were consistent with our electrophysiological findings.

We further examined the expression of KA receptor subunits in microglia in the hippocampus prepared from sham and post-ischemic rats. In the hippocampal sections prepared from sham rats, the strong immunoreactivity for GluR6/7 was observed in pyramidal cells (Fig. 4C). On the other hand, some glial cells in the stratum radiatum showed only a faint immunoreactivity for GluR6/7. In contrast, there was a strong immunoreactivity for GluR6/7 in the stratum radiatum of the hippocampal sections prepared from the animals subjected to ischemia 3 days earlier. GluR6/7-positive cells increased in the stratum radiatum were found to be mainly OX42-positive microglia (Fig. 4D, arrows).

Discussion

In the present study, we found that the responsiveness of microglia to Glu and KA was tightly regulated by the cell cycle mechanism. At the cell proliferation stage, approximately 80% of the cells exhibited Glu- and KA-induced inward currents with the mean amplitude of 13.8 ± 3.0 and 8.4 ± 0.6 pA, respectively. On the other hand, only 22.5% of the cells showed Glu- and KA-induced inward currents with the mean amplitude of 4.7 ± 0.8 and 6.2 ± 1.2 pA, respectively, at cell quiescent stage. These values were significantly smaller than those obtained at cell

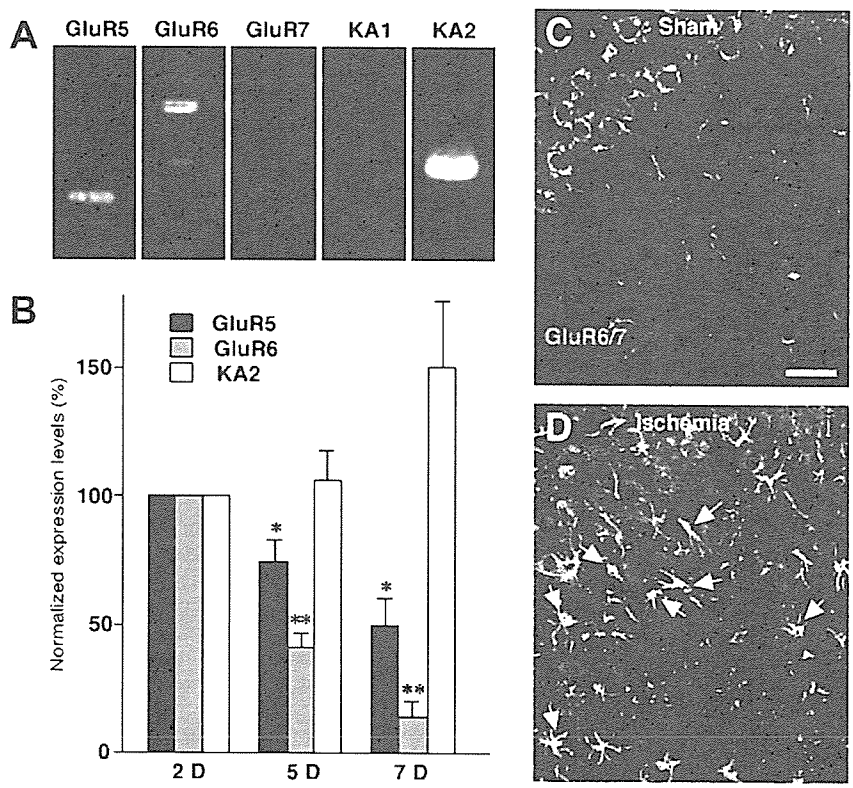

Fig. 4. Density-dependent reduction of the expression levels of KA in the GMIR1 cells. (A) RT-PCR was performed on mRNA from the GMIR1 cells to examine the expression of the KA receptor subunits mRNA. GluR5 (208 bp), GluR6 (260 bp) and KA2 (291 bp) were detected, whereas GluR7 and KA2 were not detected. (B) The normalized expression levels of GluR5. GluR6, and KA2 at 2D, 5D, and 7D by quantitative real-time RT-PCR. Each column and vertical bar represents the mean and SE of 3–4 experiments, respectively. Asterisks indicate a significant difference from 2D ($^{*}P < 0.05$, $^{**}P < 0.01$, Student's *t*-test.) (C, D) Immunofluorescent CLSM images for GluR6/7 (green) and OX42 (red) in the hippocampus prepared from animals subjected to sham-operation (C) and global ischemia (D) 3 days earlier. It was noted that some OX42 positive microglia showed intense immunoreactivities for GluR6/7 in the post-ischemic hippocampus (arrows in D). Scale bar, 100 μm.

proliferation stage. These electrophysiological observations were substantiated by the mRNA expression levels of the KA receptor subunits, GluR5 and GluR6. The expression levels of both GluR5 and GluR6 were relatively high at the cell proliferation stage, while their expression levels stayed very low at the cell quiescent stage. We also found that the immunoreactivity for GluR6/7 markedly increased in activated microglia in the post-ischemic hippocampus. Although the precise roles of the Glu receptors located on the microglia remain unclear, this cell cycle-dependent responsiveness and expression of KA receptors may have functional implications. Recently, KA has been reported to induce a rapid rearrangement of F-actin which is required for migration and phagocytic abilities of activated microglia [17]. Therefore it is reasonable to consider that Glu may induce the rearrangement of the actin cytoskeleton through the upregulated GluR5 and GluR6 during cellular proliferation.

We have also shown the microglia to have functional KA receptors because the KA-induced currents were markedly inhibited by USB296, which is a selective antagonist for the KA receptors. Furthermore, KA-responsive cells also responded to both ATPA, which is a selective agonist for GluR5. The similar results were also obtained in primary cultured rat microglia that do not increase in cell number in the absence of mitogens. ATPA also induced inward currents in the KA-responsive small population of primary cultured microglia (approximately 10% of cells). We have previously reported that KA-induced currents were potentiated by concanavalin A, which blocks desensitization of KA receptors, in some primary cultured microglia (two out of seven cells) [5]. Furthermore, Eun et al. [18] have reported that the KA-induced c-fos gene expression in primary cultured rat microglia was not potentiated in the presence of cyclothiazide, which is known to potentiate AMPA-induced currents by inhibiting the desensitization of AMPA receptors. These observations further support our finding that the microglia have functional KA receptors. More recently, however, Hagino et al. [19] demonstrated that the KA-induced currents in primary cultured rat microglia were mostly AMPA receptor-mediated currents while the KA receptors were barely functional. This conclusion was mainly based on their finding that the KA-induced currents were completely inhibited by LY300164 at a concentration of 100 μM, a selective inhibitor for AMPA receptors. However, IC_{50} of LY300164 for AMPA and KA receptors were originally reported to be 1.7 μM and 2.6 μM, respectively [20]. Therefore, it is reasonable to consider that LY300164 at a concentration of 100 μM could therefore suppress the responses mediated by both AMPA and KA receptors.

In conclusion, microglia were thus found to have functional KA receptors, mainly consisting of GluR5 and GluR6, and the expression levels of these subunits are closely regulated by the cell cycle mechanism.

Acknowledgments

This study was supported by Grant-in-Aid for Scientific Research on Priority Area (No. 15082204) for that Ministry of Education, Science and Culture, Japan (H.N.).

References

[1] K. Färber, H. Kettenmann, Physiology of microglial cells, Brain Res. Rev. 48 (2005) 133–143.
[2] Y. Hayashi, H. Ishibashi, K. Hashimoto, H. Nakanishi, Potentiation of the NMDA receptor-mediated responses through the activation of the glycine site by microglia secreting soluble factors, Glia 53 (2006) 660–668.
[3] C. Matute, M. Domercq, M-V. Sánchez-Gómez, Glutamate-mediated glial injury: mechanisms and clinical importance, Glia 53 (2006) 212–224.
[4] S. Moriguchi, Y. Mizoguchi, Y. Tomimatsu, Y. Hayashi, T. Kadowaki, Y. Kagamiishi, N. Katsube, K. Yamamoto, K. Inoue, S. Watanabe, J. Nabekura, H. Nakanishi, Potentiation of NMDA receptor-mediated synaptic responses by microglia, Mol. Brain Res. 119 (2003) 160–169.
[5] M. Noda, H. Nakanishi, J. Nabekura, N. Akaike, AMPA-kainate subtypes of glutamate receptor in rat cerebral microglia, J. Neurosci. 20 (2000) 251–258.
[6] M. Gottlieb, C. Matute, Expression of ionotropic glutamate receptor subunits in glial cells of the hippocampal CA1 area following transient forebrain ischemia, J. Cereb. Blood Flow. Metab. 17 (1997) 290–300.
[7] H. Kato, A. Takahashi, Y. Itoyama, Cell cycle expression in proliferating microglia and astrocytes following transient global cerebral ischemia in the rat, Brain Res. Bull. 60 (2003) 215–221.
[8] H. Ino, T. Chiba, Cyclin-dependent kinase 4 and cyclin D1 are required for excitotoxin-induced neuronal cell death in vivo, J. Neurosci. 21 (2001) 6086–6094.
[9] K. Salimi, K. Moser, B. Zassler, M. Reind, N. Embacher, C. Schermer, C. Weis, J. Marksteiner, M. Sawada, C. Humpel, Glial cell line-derived neurotrophic factor enhances survival of GM-CSF dependent rat GMIR1-microglial cells, Neurosci. Res. 43 (2002) 221–229.
[10] K. Koguchi, Y. Nakatsuji, T. Okuno, M. Sawada, S. Sakoda, Microglial cell cycle-associated proteins control microglial proliferation in vivo and in vitro and are regulated by GM-CSF and density-dependent inhibition, J. Neurosci. Res. 74 (2003) 898–905.
[11] D.F. Sastradipura, H. Nakanishi, T. Tsukuba, K. Nishishita, H. Sakai, Y. Kato, T. Gotow, Y. Uchiyama, K. Yamamoto, Identification of cellular compartment involved in processing of cathepsin E in primary cultures of rat microglia, J. Neurochem. 70 (1998) 2045–2056.
[12] H. Nakanishi, T. Tsukuba, T. Kondou, T. Tanaka, K. Yamamoto, Transient forebrain ischemia induces expression and specific localization of cathepsins E and D in rat hippocampus and neostriatum, Exp. Neurol. 121 (1993) 215–223.
[13] Y. Hayashi, Y. Tomomatsu, H. Suzuki, J. Yamamda, Z. Wu, H. Yao, Y. Kagamiishi, N. Tateishi, M. Sawada, H. Nakanishi, The intra-arterial injection of microglia protects hippocampal CA1 neurons against global ischemia-induced functional deficits in rats, Neuroscience, in press.
[14] J.C. More, R. Nistico, N.P. Dolman, V.R. Clarke, A.J. Alt, A.M. Ogden, F.P. Buelens, H.M. Troop, E.E. Kelland, F. Pilato, D. Bleakman, Z.A. Bortolotto, G.L. Collingridge, D.E. Jane, Characterisation of UBP296: a novel, potent and selective kainate receptor antagonist, Neuropharmacology 47 (2004) 46–64.
[15] V.R. Clarke, B.A. Ballyk, K.H. Hoo, A. Mandelzys, A. Pellizzari, C.P. Bath, J. Thomas, E.F. Sharpe, C.H. Davies, P.L. Ornstein, D.D. Schoepp, R.K. Kamboj, G.L. Collingridge, D. Lodge, D. Bleakman, A hippocampal GluR5 kainate receptor regulating inhibitory synaptic transmission, Nature 389 (1997) 599–603.

[16] M. Frerking, R.A. Nicoll, Synaptic kainate receptors, Curr. Opin. Neurobiol. 10 (2000) 342–351.
[17] R.N. Christensen, B.K. Ha, F. Sun, J.C. Bresnahan, M.S. Beattie, Kainate induces rapid redistribution of the actin cytoskeleton in ameboid microglia, J. Neurosci. Res. 84 (2006) 170–181.
[18] S.Y. Eun, Y.H. Hong, E.H. Kim, H. Jeon, Y.H. Suh, J.E. Lee, C. Jo, S.A. Jo, J. Kim, Glutamate receptor-mediated regulation of c-fos expression in cultured microglia, Biochem. Biophys. Res. Commun. 325 (2004) 320–327.
[19] Y. Hagino, Y. Kariura, Y. Manago, T. Amano, B. Wang, M. Sekiguchi, K. Nishikawa, S. Aoki, K. Wada, M. Noda, Heterogeneity and potentiation of AMPA type of glutamate receptors in rat cultured microglia, Glia 47 (2004) 68–77.
[20] G. Abraham, S. Solyom, E. Csuzdi, P. Berzsenyi, I. Ling, I. Tarnawa, T. Hamori, I. Pallagi, K. Horvath, F. Andrasi, G. Kapus, L.G. Harsing Jr., I. Kiraly, M. Patthy, G. Horvath, New non competitive AMPA antagonists, Bioorg. Med. Chem. 8 (2000) 2127–2143.

Available online at www.sciencedirect.com
ScienceDirect
Neuroscience Research 56 (2006) 294–299
Neuroscience Research
www.elsevier.com/locate/neures

Amyloid-β peptides induce several chemokine mRNA expressions in the primary microglia and Ra2 cell line via the PI3K/Akt and/or ERK pathway

Sachiko Ito [a], Makoto Sawada [b], Masataka Haneda [a], Yoshiyuki Ishida [c], Ken-ichi Isobe [a,*]

[a] *Department of Immunology, Nagoya University Graduate School of Medicine, 65 Turumai-cho, Showa-ku, Nagoya, Aichi 466-8520, Japan*
[b] *Department of Brain Life Science, Research Institute for Environmental Medicine, Nagoya University, Furo-cho, Chikusa-ku, Nagoya 464-8601, Japan*
[c] *Radioisotope Research Center, Nagoya University, Furo-cho, Chikusa-ku, Nagoya 464-8601, Japan*

Received 11 April 2006; accepted 26 July 2006
Available online 15 September 2006

Abstract

Alzheimer's disease (AD) is characterized by the presence of senile plaques composed primarily of amyloid-β peptide (Aβ) in the brain. Microglia have been reported to surround these Aβ plaques, which have opposite roles, provoking a microglia-mediated inflammatory response that contributes to neuronal cell loss or the removal of Aβ and damaged neurons. To perform these tasks microglia migrate to the sites of Aβ secretion. We herein analyzed the process of chemokine expression induced by Aβ stimulation in primary murine microglia and Ra2 microglial cell line. We found that Aβ1-42 induced the expressions of CCL7, CCL2, CCL3, CCL4 and CXCL2 in the microglia. The signal transduction pathway for the expression of CCL2 and CCL7 mRNA induced by Aβ1-42 was found to depend on phosphatidylinositol 3-kinase (PI3K)/Akt and extracellular signal-regulated kinase (ERK), whereas the pathway for CCL4 depended only on PI3K/Akt. These inflammatory chemokine expressions by Aβ stimulation emphasize the contribution of neuroinflammatory mechanisms to the pathogenesis of AD.

Keywords: Microglia; Alzheimer's disease; Amyloid β; Chemokine; Akt; ERK

1. Introduction

Alzheimer's disease (AD) is characterized by the presence of senile plaques composed primarily of amyloid-β peptide (Aβ) in the brain. Microglia have been reported to surround Aβ plaques (Haga et al., 1989; Itagaki et al., 1989). Aβ-induced microglia have been shown to produce reactive oxygen species, TNFα, IL1β, which have been demonstrated to cause the degeneration of nervous cells (Akiyama et al., 2000; Ishii et al., 2000; Blasko et al., 2004). On the other hand, microglia play an important role in the clearance of Aβ by phagocytosis, primarily through scavenger receptor class A (SR-A, CD204), scavenger receptor-BI (SR-BI) and CD36 (El Khoury et al., 1996; Paresce et al., 1996; Husemann et al., 2002). Other receptors such as receptor for advanced glycosylation end-products (RAGE), integrins and heparan sulfate proteoglycans, have also been reported to bind with Aβ (Verdier and Penke, 2004). CD36 binds to Aβ *in vitro* (Bamberger et al., 2003), and it is physically associated with members of the Src family tyrosine kinase (Huang et al., 1991; Bull et al., 1994), which transduce signals from this receptor (Jimenez et al., 2000).

Microglia as a macrophage-lineage cell may produce several chemokines, which induce microglial chemotaxis. It has recently been reported that microglia produce MCP-1 (CCL2) and other chemokines by Aβ stimulation through CD36 receptor (El Khoury et al., 2003). Another report examined the production of chemokines in THP-1 monocytes

Abbreviations: AD, Alzheimer's disease; Aβ, amyloid-β; ERK, extracellular signal-regulated kinase; FBS, fetal bovine serum; GM-CSF, granulocyte-macrophage colony stimulating factor; PBS, phosphate-buffered saline; PI3K, phosphatidylinositol 3-kinase

* Corresponding author. Tel.: +81 52 744 2135; fax: +81 52 744 2972.
E-mail address: kisobe@med.nagoya-u.ac.jp (K.-i. Isobe).

0168-0102/$ – see front matter
doi:10.1016/j.neures.2006.07.009